Astrophysical and Terrestrial Constraints on Yukawa Potentials

A thesis submitted in partial fulfillment of the requirement
for the degree of Bachelor of Science with Honors in
Physics from the College of William and Mary in Virginia,

by

James Younkin

Accepted for Honors

Advisor: Prof. Marc Sher

Prof. James Woodbridge

Prof. Henry Krakauer

Williamsburg, Virginia
May 2004

Contents

Acknowledgments

I would like to thank my advisor Dr. Marc Sher for spending so much time answering my questions and pointing me in new directions, and I would also like to thank Laura Hanscom for her continuous support. Without them, this research would not have been possible.

List of Figures

List of Tables

Abstract

Great effort has been put into probing the universe for new forces beyond the standard model. Researchers mainly concentrate on forces that arise from possible, but not yet detected, consequences of particle theories. One such construct is the Yukawa potential. In this study, we will concentrate on deriving constraints for the parameters of the Yukawa potential in three different systems — the Sun-Earth system, a binary pulsar, and a terrestrial free-fall experiment.

Chapter 1

Introduction

1.1 Fifth Forces and the Yukawa Potential

Newton's Law of gravitational attraction was formulated by studying the apparent behavior of objects. By continuing this study we may find new forces, so-called *fifth forces*, that have previously gone unnoticed. Discounting relativity, the goal of studying fifth forces — very small modifications to Newtonian gravity — is to use phenomena to build constraints on possible additions to the gravitational potential[8]. This is not only a useful test of our theories of gravity, but an important look into possible extensions of the Standard Model of particle physics. Some proposed particles and symmetries would create forces much weaker than gravity, and constraints on these effects will rule out possible theories. When these theories are ruled out, particle physics is able to concentrate on more probable solutions to the current deficiencies in its models.

In this study, we will focus on a single (and extremely important) type of potential, called a *Yukawa potential*. This potential is associated with the exchange of scalar or vactor bosons [24]; currently, these are very important because they are associated with the Higgs mechanism, axions, and most other proposed additions to current theory. We will concentrate exclusively on the potential associated with scalar bosons,

and so we use the terms "Yukawa potential" and "scalar potential" interchangeably. In general, the form of this potential is

$$V(r) = \frac{-\alpha e^{-\frac{r}{\lambda}}}{r}$$

but since we will work with them in the context of gravity, we accept the standard convention and redefine α so that

$$V(r) = \frac{-\alpha G m_1 m_2 e^{-\frac{r}{\lambda}}}{r} \tag{1.1}$$

This is the equation for the additional potential energy between two bodies due to the presence of the scalar potential. In this equation, α is called the *coupling constant* or *strength* of the potential; λ is often referred to as the range, but in this paper it will be referred to as the *distance scale* of the potential. Note that in the case of scalar potentials, the coupling constant in (1.1) is greater than zero [8].

1.2 Current Research on Fifth Forces

A large amount of research into constraints on these parameters has already been conducted. Figure 1.1 summarizes the work to date. The shaded areas are the parameter values ruled out by current experimental evidence. Note that the constraints in figure 1.1 asssume a scalar potential which couples to mass uniformly — this type of potential is called *composition-independent*.

In addition to studying this type of potential, we will also investigate *composition-dependent* potentials. The strength of a composition-dependent potential depends on the properties of the mass to which it couples. Among the properties that the coupling strength can depend on are isospin (neutron number minus proton number), baryon number (total number of nucleons), and a few other nuclear properties. These forces will create measurable differences in the gravitational accelerations of unlike

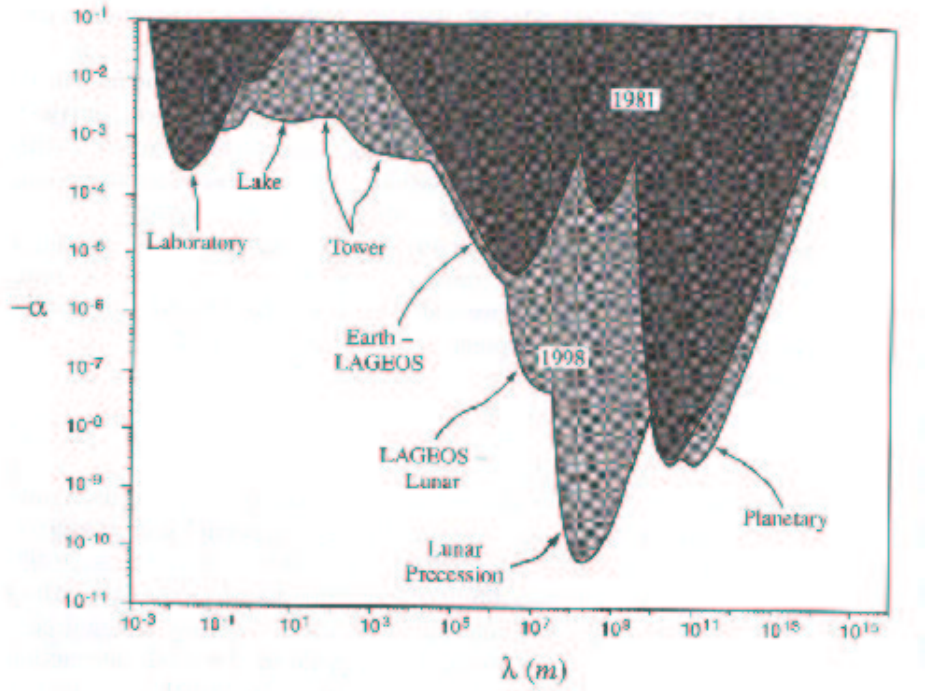

Figure 1.1: Constraints on the Yukawa Potential as of 1998

masses. Although all scalar interactions will in principle be composition-dependent [5], coupling to mass will effectively be composition-independent at large distance scales because, as we shall soon see, significant composition-dependent effects are only possible at very short ranges.

1.2.1 Composition-Independent Constraints

In order to understand how this research fits into the larger project to discover the constraints on forces weaker than gravity, we will now briefly summarize the work performed to date [8]. The first half of the research investigates composition-independent forces, and we shall survey this work by working our way across figure 1.1 from short to long distance scales.

The first distance scale range is the laboratory range, which involves all fifth

forces with distance scales less than one meter. The work that represents the best constraints in this range was performed by Spero and Hoskins *et. al.* [20] [10]; Spero *et. al.* have produced constraints in the 2-5cm region, and Hoskins *et. al.* have studied the 5-105cm region. Both used torsion balances in different setups to search for anomalous effects. These are null experiments; in other words, they are set up so that zero-effect measurements correspond to ordinary Newtonian gravity.

Figure 1.2 illustrates how the basic torsion balance experiment works. In Spero *et al*'s experiment, a test mass is placed inside a homogeneous metal cylinder and enclosed in a thermally and magnetically shielded vacuum chamber. Given a standard inverse-square force between the test mass and an infinite cylinder, there will be no net effect on the torsion balance (the experimenters made special adjustments for the fringe fields at the end of the cylinder). But a weak non-Newtonian potential will create a net force on the mass. In response to this force, there would be a net torque about the tungsten wire, and the experimental apparatus would begin precessing. This motion would be picked up in tandem by the optical and electrostatic sensors. The experiment produces a null result; Spero *et. al.* find no evidence for deviations from Newtonian gravity. A Yukawa potential at the relevant distance scale is thus constrained to produce an effect within the experimental error; the region excluded produces effects which are beyond two standard deviations of the null result.

Hoskins *et. al.*'s experiment is a slight modification of this setup. The test mass of the torsion balance is on a small track and interacts with another mass on a track across a room. The near mass and the far mass are chosen so that the regular Newtonian interaction between the two as they are moved along the tracks produces no effect on the torsion balance. But a non-Newtonian force will produce a net torque on the torsion balance that can be measured by the apparatus's sensors. Again a null result was found, and the experimental error constrains a Yukawa potential over the

corresponding distance scale.

There are several difficulties confronting experiments dealing with these distances. Primarily, they must control non-gravitational forces acting on the experimental setup. The torsion balances in these experiments had to be shielded from outside interference from electromagnetic effects and be enclosed in a vacuum, for instance. These effects are responsible for the experimental uncertainty, and can be quite difficult to control. One experiment by Long that purportedly suggested the existence of a force in this range, but it was later found that his floor was slightly tilted, which was the source of the anomalous effect [8].

It is even more difficult to constrain potentials whose distance scale is within the so-called "geophysical window", which corresponds to ranges between one meter and one hundred kilometers. In this range, experimental tests for non-Newtonian gravity involve some sort of interaction with a geological formation or the earth itself. Although other types of experiments have been performed, the best constraints on potentials in this region are currently provided by lake and tower experiments.

The lake experiment of Hubler *et. al.* provides the next region of constraint on Yukawa potentials. This type of experiment is performed next to a body of water and measures the force on two different separated masses.

The lake used is actually a reservoir, and so the water level can be raised and lowered, as shown in figure 1.3. By comparing measurements of the force due to the mass of the lake at different water levels, any fifth-force can be separated from the predicted gravitational force. As with the torsion balance experiments, no anomalous effect was detected, and the experimental error determines the "lake" portion of the curve in figure 1.1.

The most precise tower experiment was performed by Romaides *et. al.* in 1994 [18]. Tower experiments measure the gravitational acceleration due to the Earth at

various heights up a tall tower. The key to this type of experiment is an accurate survey of the local terrain; because measurements are being taken very close to the Earth's surface, variations in local mass densities would be read as an anomalous effect if not accounted for. In this experiment, a 610m tall tower in Inverness, MS was specifically chosen because it was in the middle of a very flat clearing. Romaides *et. al.* had to be extremely thorough in taking accurate surveys of the area surrounding the site, especially around the base of the tower. After taking measurements at five different heights and accounting for local features, they were able to constrain Yukawa-type potentials to within experimental error.

Perhaps the most striking feature of the current bounds is how relatively weak the constraints are in the geophysical window. This is due to the tremendous difficulties one encounters when attempting to study interactions between a test mass and the Earth. In order to measure this gravitational effect with high precision, it is imperative that the density and shape of the local area be known to equally high precision. For instance, if there were a giant iron deposit near the tower in Inverness, the net gravitational pull of the Earth would be slightly different than expected because of the relatively large effect of this local inhomogeneity. Experiments involving water are at a slight advantage here; finding the density of a standing body of water is not much of a problem. However, one must still take into account the terrain surrounding the water. Although experiments measuring the force of gravity in the ocean have been attempted, they are not as accurate because of the poorly understood features of the ocean floor [25].

Constraints at higher distance scales are provided by satellite and astrophysical observations. The first range, spanning the Earth-LAGEOS and LAGEOS-Lunar areas of figure 1.1, is made up of two types of observations of the Earth-Moon system made with the help of the LAGEOS satellites. LAGEOS 1 and 2, the LAser GEOdy-

namics Satellites, are two perfectly spherical satellites designed to reflect laser beams from stations on the Earth [17]. Reception of the reflected signals allows for ranging accurate to within three centimeters. This incredibly accurate rangefinding makes these two observations possible.

The Earth-LAGEOS observation is a measurement of the LAGEOS 1 satellite's orbit performed by Smith *et. al.* [19]. There are 80 Earth-based stations placed around the world that are designed to take laser rangefinding measurements of the satellite. In this particular observation, ranges were taken continuously over a series of days, resulting in hundreds of thousands of accurate distance measurements. From this data, the orbital parameters of the satellite may be inferred to high accuracy. In their analysis, Smith *et. al.* use this to determine the product of the gravitational constant and the mass of the Earth to a precision of $\pm 0.002 \frac{km^3}{s^2}$. Now the Yukawa potential may be interpreted as a position-dependent gravitational constant; taking the sum of a Yukawa potential and the normal gravitational potential, we find

$$\begin{aligned} \frac{G(r)M_E m_S}{r} &= \frac{G_o M_E m_S}{r}(1+\alpha e^{-\frac{r}{\lambda}}) \\ G(r) &= (1+\alpha e^{-\frac{r}{\lambda}}) \end{aligned}$$

Since no anomalous effects were detected in the orbit of the satellite, a Yukawa potential is constrained within the observational uncertainty, as shown in figure 1.1.

The LAGEOS-Lunar measurement was much more difficult from a technical standpoint [6]. The Apollo 11, 14, and 15 missions carried corner-cube retroreflector arrays to the Moon and placed them at widely spaced intervals. These arrays, along with one placed on a Soviet rover, are entirely passive and are designed to reflect electromagnetic radiation. Despite the fact that the intensity decreases by 10^{-21} in reflection from the Earth to the Moon and back, stations on the Earth designed to distinguish single-photon signals are able to make rangefinding measurements that are accurate

to within 10 centimeters. Using these signals and reflections from the LAGEOS satellites, Dickey *et. al.* were able to accurately determine the orbital parameters of the Moon in the Earth-Moon system. One result of these calculations was a constraint on violations of the Weak Equivalence Principle - the result of such violations would be a shift in the center of the Moon's orbit towards the Sun. As noted above, violations of the WEP may simply be restated in terms of a fifth-force, and so this constraint on violations of the WEP also puts a constraint on the parameters of a Yukawa potential. The results of the analysis of these observations make up the LAGEOS-Lunar portion of figure 1.1.

The planetary region of the constraint curve comes from measurement of the periastron precession of Mars and Mercury (see sections 3.1 – 3.3 for more details). Simple astronomical observation of the orbits of these planets allows us to make measurements of this anomalous effect. The precession is a result from General Relativity; being free-falling objects, the planets move in the geodesics of the Schwarzschild metric whose central gravitating mass is the Sun [3]. In the weak field limit, these geodesics will correspond to ordinary Keplerian orbits. However, because the masses in a Sun-Planet system are so large, a non-Keplerian element of the geodesic manifests itself, and the planet's orbit will rotate in the orbital plane. This effect, known as the precession of the periastron, is given by

$$\Delta\phi = \frac{6\pi G^2 M^2}{L^2}$$

We are able to constrain a Yukawa potential to the accuracy that we can measure this effect because this potential will create an *additional* precession. Observations of the precessions of Mars and Mercury make up the remainder of figure 1.1 [8]. A reader confused by this paragraph should not worry; much more will be said on this topic in Chapter 3.

1.2.2 Composition-Dependent Constraints

The principal tests that are used to constrain composition-dependent scalar potentials are torsion balance and free-fall experiments. Each of these has its advantage - torsion balances are more sensitive, but free-fall experiments are able to provide constraints for a more extensive range of distance scales [8]. The composition-dependent torsion balance experiment is also called an Eötvös experiment; a good example of this type of experiment was performed by Boynton *et. al.* in 1987 [2] - the experimental setup is given in figure 1.4. This experiment uses a modified torsion balance; instead of a lever arm, it has an aluminum-beryllium ring hanging from the torsion wire. The experimental assembly is placed four meters inside the face of a 330-meter-tall cliff in Washington State. The tunnel into the cliff is monitored for constant temperature, magnetically shielded by Helmholtz coils, and sealed from the outside air. Calibration allows the experimenters to determine the initial tilt on the assembly due to the mass distribution inside the cliff. In the presence of a non-Newtonian composition-dependent potential, the aluminum-beryllium ring becomes a dipole. The apparatus is rotated so that the dipole axis is perpindicular to the cliff face (i.e., one side of the ring faces toward the cliff and the other faces away) and small oscillations of the torsion balance are measured. A signal was discovered offering possible evidence for a fifth force coupling primarily to isospin (neutron number minus atomic number) at distance scales $20m < \lambda < 1km$, but further experimentation is required in this area.

A second type of test is the free-fall experiment, also known as a Galilean experiment. In these experiments, objects of different composition but identical inertial mass are dropped to determine if they fall at the same rate. This is really just a direct test of the Weak Equivalence Principle; if the objects fall at exactly the same rate, inertial and gravitational mass are identical and there can be no modification of Newtonian gravity. We will have much more to say on this type of experiment in

Chapter 2.

1.2.3 Concluding Remarks

In this paper, we will seek to expand upon this research by studying two systems which constrain composition-independent potentials and one which constrains a composition-dependent potential. We first investigate whether measuring a shift in the Earth-Sun Lagrange points can create useful constraints on a Yukawa potentials with distance scales between 10^5 and 10^7 kilometers. Our second system will be the binary pulsar B1913+16; we will calculate the constraint created by the precession of its periastron. Finally we will study the constraints placed on a specific composition-dependent potential by a Galilean free-fall experiment performed in 1992.

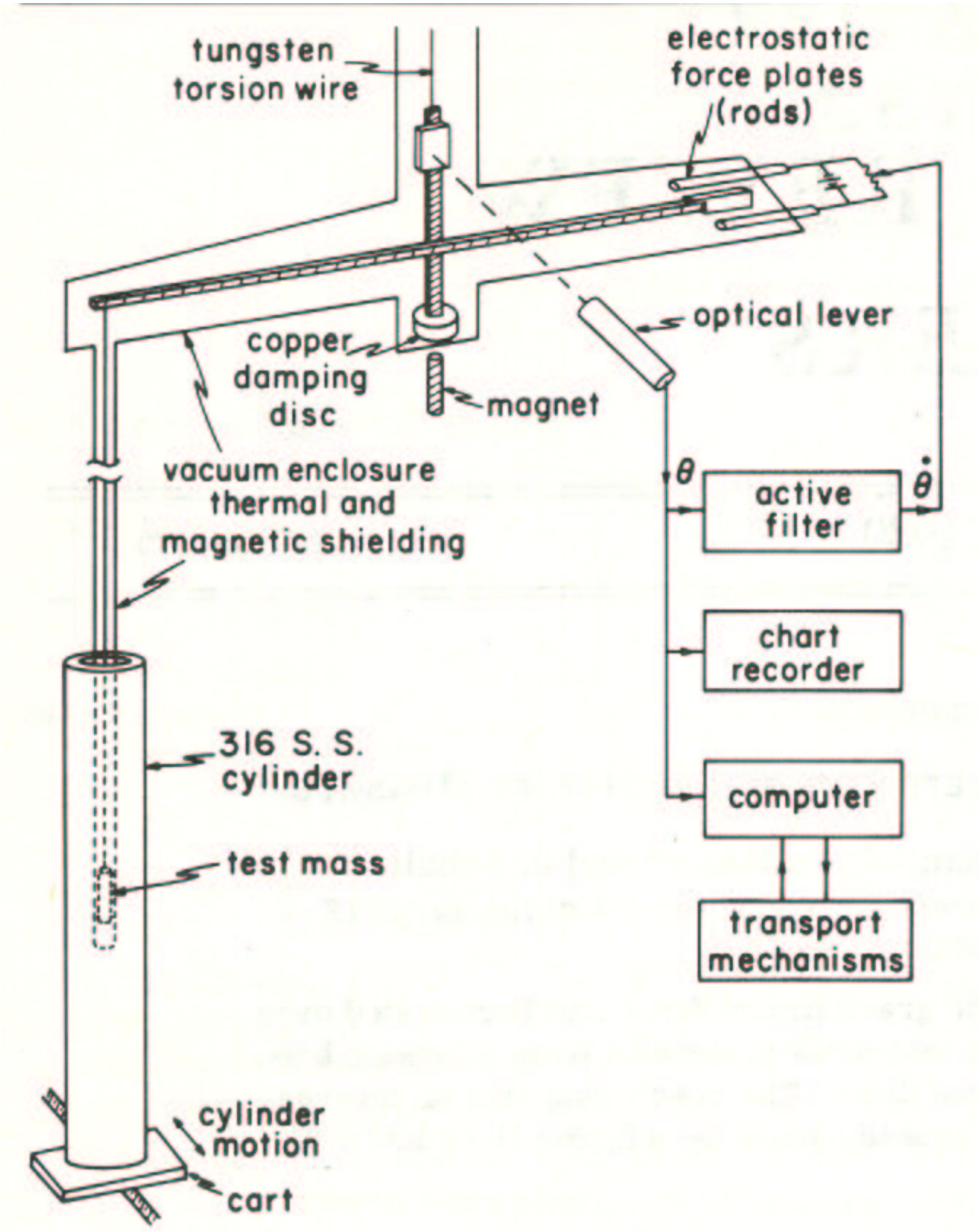

Figure 1.2: Experimental Setup of Spero *et. al.* [20]

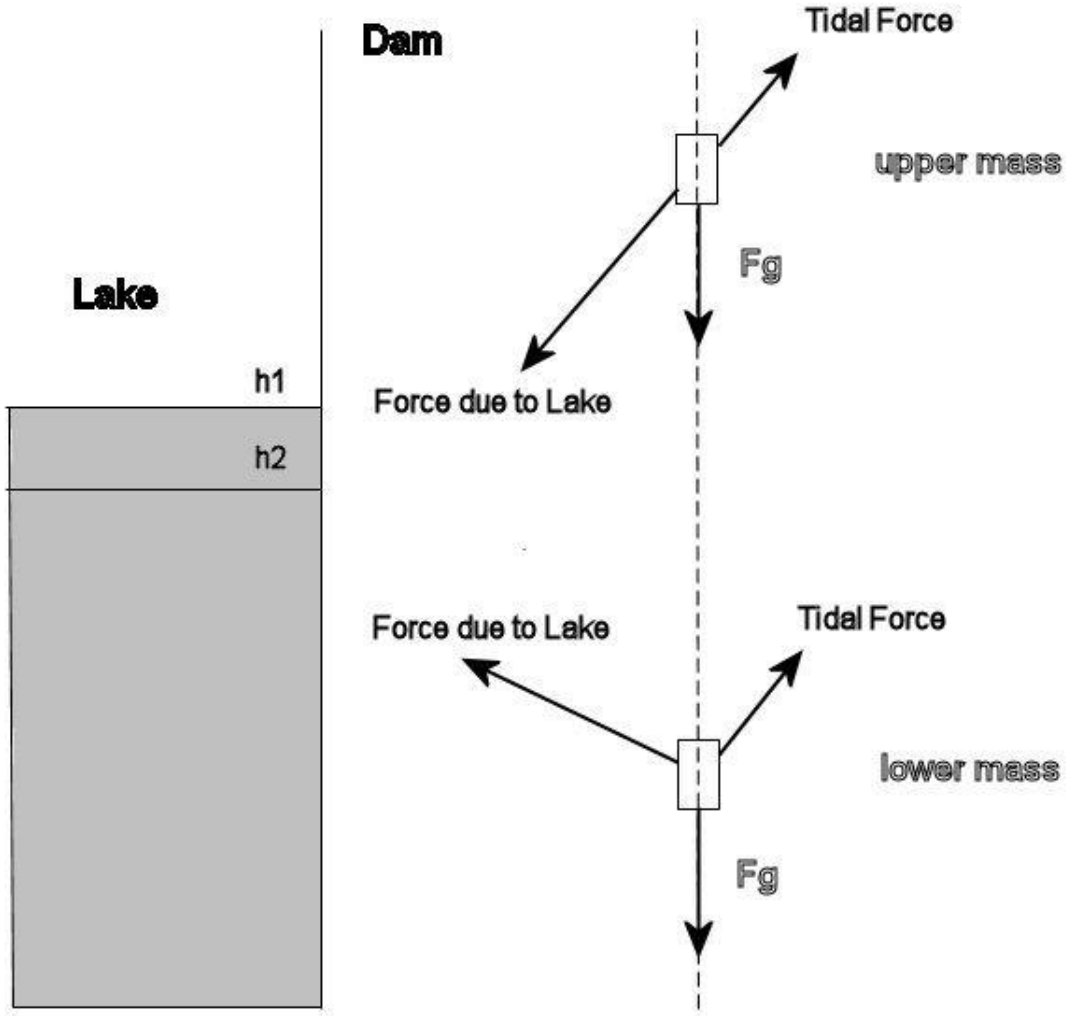

Figure 1.3: Lake Experiment of Hubler *et. al.* [11]

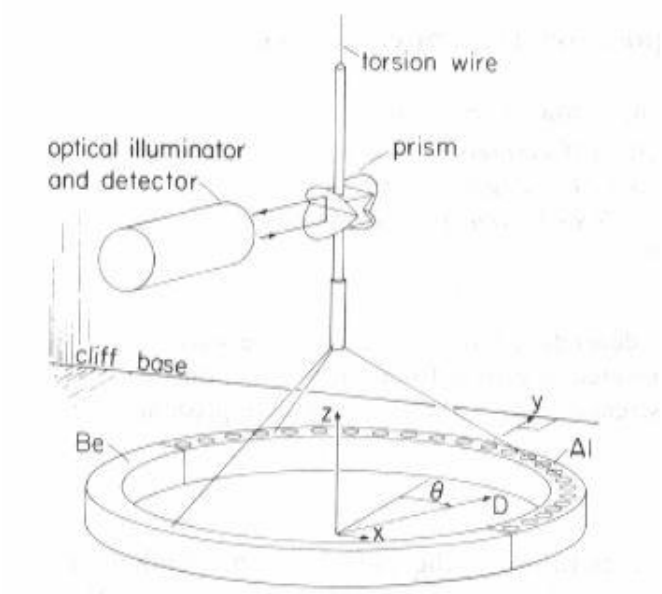

Figure 1.4: Experimental Setup of Boynton *et. al.* [2]

Chapter 2

Shift in Lagrange Orbital Points Due to a Scalar Potential

2.1 Lagrange Points

Consider a two-body system in which one mass is very much larger than the other. Then the center of the heavier body, which we will call the *central body*, will be approximately at the center of mass of the system, and the lighter body, which we call the *orbiting body*, will appear to orbit it. Assume that the orbit of this body is circular, or approximately so. In this system, there exist five orbital points called *Lagrange points* [1]. The significance of these points is that objects placed at these locations will remain at the same position relative to the orbiting body provided there is no force to disturb this equilibrium. Appropriately, these five points are named L1, L2, L3, L4, and L5, and their positions are shown in figure 2.1 below. L1, L2, and L3 are on the line intersecting the centers of the two bodies: L1 is a small distance from the orbiting body, between the central and orbiting bodies; L2 is a short distance from the orbiting body on its far side; and L3 is on the intersection of this line and the circle formed by the orbit. L4 and L5 are also located on the circle that the orbit forms. Consider the line segment whose endpoints are the center of the two bodies and then construct two equilateral triangles whose base is this line segment and whose

apex is on the orbit's circle. These two apices are the L4 and L5 orbital points. L4 is defined to be the point *ahead* of the orbiting body in its orbit and L5 is defined to be the point *behind* it.

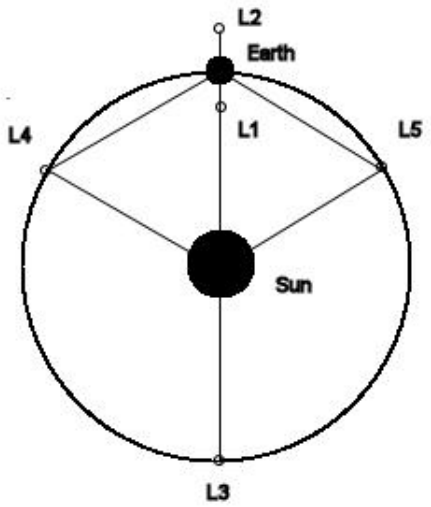

Figure 2.1: The Lagrange points of the Sun-Earth system

We are interested in these points in the context of the Earth-Sun system. This system is essentially two-body since the small effects of the gravitational fields of nearby planets may be ignored. If a scalar potential is added to the system, the positions of these orbital points will change. By measuring the actual distance from the Earth to an object orbiting at a Lagrange point it would be possible put an observational constraint on a change in that point's position. This limit would dictate the maximum potential strength allowed for a given distance scale and therefore the types of possible scalar potentials. In this study we will concentrate on the L2 point for the reason that the WMAP (Wilkinson Microwave Anisotropy Probe) has been put in orbit around it, and distance measurements would, presumably, have been taken at regular intervals[16].

Calculating the location of Lagrange points involves finding locations in the two-dimensional plane formed by the system where a third body can orbit the central body with the same period as the orbiting body. Finding the L4 and L5 points is rather difficult, but the three others are not very hard because, as was stated before, the two bodies and the orbital point are located on the same line. It can be shown (using the methods developed below) that the distance from the Earth to the L2 Earth-Sun Lagrange point is given by

$$\frac{1}{(r+R)^3} + \frac{\mu}{R^2(r+R)} = \frac{1}{r^3} \tag{2.1}$$

where r is the distance from the Sun to the Earth, R is the distance from the Earth to L2, and μ is defined as the ratio of the Earth's mass to the Sun's mass. This unperturbed distance turns out to be about 1.5 million kilometers. Later, when we have an equation for the perturbed distance to L2, we will use equation (2.1) to define the distance that the point is shifted by the presence of the scalar potential. We now turn our attention to that calculation.

2.2 Calculating the Shifted Location of L2

Our goal in this analysis is to determine whether measuring the distance to the L2 Lagrange point will produce a useful constraint on a composition-independent scalar potential. As we noted above, the Lagrange point will be located at the point where the combined forces on a test object from the central body and the orbiting body cause that test object to orbit the central body *with the same orbital period* as the orbiting body itself. This is the requirement which causes an object at that location to remain in the same relative position to the orbiting body. Define r to be the distance from the Sun to the Earth, and define R to be the modified distance from the Earth to the L2 point. Note that in the distance scales we are considering

here, $10^5 km \leq \lambda \leq 10^7 km$, the force on the Earth due to the Sun is negligible and r is therefore a constant in this calculation. We do, however, include the (small) modification in the rotational period of the Earth.

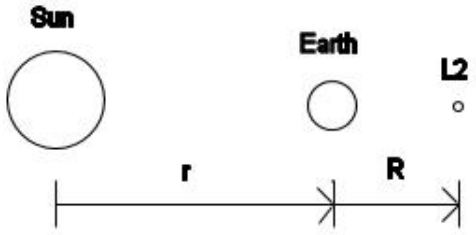

Figure 2.2: Diagram of the L2 calculation

As discussed before, α is defined so that the form of our scalar potential is

$$V_\alpha(r) = -\frac{\alpha G M m}{r} e^{-\frac{r}{\lambda}}$$

The modified force on the Earth due to the Sun is

$$\begin{aligned} F &= \frac{G M_E M_S}{r^2} - \frac{d}{dr}\{\frac{\alpha G M_E M_S}{r} e^{-\frac{r}{\lambda}}\} \\ F &= \frac{G M_E M_S}{r^2} + \frac{\alpha G M_E M_S}{r^2} e^{-\frac{r}{\lambda}} + \frac{\alpha G M_E M_S}{r\lambda} e^{-\frac{r}{\lambda}} \\ F &= \frac{G M_E M_S}{r^2}[1 + \alpha(1 + \frac{r}{\lambda}) e^{-\frac{r}{\lambda}}] \end{aligned}$$

Because this is the central force keeping the Earth in orbit and the α term is small,

we may equate this force to $\frac{M_E v^2}{r}$, which leads to

$$v_E{}^2 = \frac{GM_S}{r}[1 + \alpha(1 + \frac{r}{\lambda})e^{-\frac{r}{\lambda}}]$$

Now define T_E as the modified orbital period of the Earth. Because the Earth's orbit is very nearly circular, we may use

$$\begin{aligned} v_E &= \frac{2\pi r}{T_E} \\ v_E{}^2 &= \frac{4\pi^2 r^2}{T_E{}^2} \end{aligned}$$

Substitution for $v_E{}^2$ then yields

$$\frac{4\pi^2}{T_E{}^2} = \frac{GM_S}{r^3}[1 + \alpha(1 + \frac{r}{\lambda})e^{-\frac{r}{\lambda}}] \tag{2.2}$$

Now consider a test object of mass m orbiting the Earth at the L2 point. Then by definition its distance from the central body is $r + R$. The total force on the mass is given by

$$F = \frac{GM_S m}{(r+R)^2} - \frac{d}{dr}V_{\alpha_S}(r+R) + \frac{GM_E m}{R^2} - \frac{d}{dr}V_{\alpha_E}(R)$$

where $V_{\alpha_S}(r+R)$ is the scalar potential due to the Sun, and $V_{\alpha_E}(R)$ is the scalar potential due to Earth. Now, as in the previous results, we find

$$F = \frac{GM_S m}{(r+R)^2}[1 + \alpha(1 + \frac{r+R}{\lambda})e^{-\frac{r+R}{\lambda}}] + \frac{GM_E m}{R^2}[1 + \alpha(1 + \frac{R}{\lambda})e^{-\frac{R}{\lambda}}]$$

To remain in the same position relative to the Earth, the test object must move in a nearly circular orbit as well. So we set this force equal to $\frac{mv^2}{r+R}$ and obtain

$$v^2 = \frac{GM_S}{r+R}[1 + \alpha(1 + \frac{r+R}{\lambda})e^{-\frac{r+R}{\lambda}}] + \frac{GM_E(r+R)}{R^2}[1 + \alpha(1 + \frac{R}{\lambda})e^{-\frac{R}{\lambda}}]$$

Now define T as the orbital period of the test object and substitute for v^2

$$v^2 = \frac{4\pi^2(r+R)^2}{T^2}$$

$$\frac{4\pi^2(r+R)^2}{T^2} = \frac{GM_S}{r+R}[1+\alpha(1+\frac{r+R}{\lambda})e^{-\frac{r+R}{\lambda}}] + \frac{GM_E(r+R)}{R^2}[1+\alpha(1+\frac{R}{\lambda})e^{-\frac{R}{\lambda}}]$$

$$\frac{4\pi^2}{T^2} = \frac{GM_S}{(r+R)^3}[1+\alpha(1+\frac{r+R}{\lambda})e^{-\frac{r+R}{\lambda}}] + \frac{GM_E}{R^2(r+R)}[1+\alpha(1+\frac{R}{\lambda})e^{-\frac{R}{\lambda}}] \qquad (2.3)$$

Now, as was noted before, the test object must have the same period as the Earth to remain in the same relative position over the entire orbit. This condition is expressed by equating (2.2) and (2.3):

$$\frac{GM_S}{r^3}[1+\alpha(1+\frac{r}{\lambda})e^{-\frac{r}{\lambda}}] = \frac{GM_S}{(r+R)^3}[1+\alpha(1+\frac{r+R}{\lambda})e^{-\frac{r+R}{\lambda}}]+\frac{GM_E}{R^2(r+R)}[1+\alpha(1+\frac{R}{\lambda})e^{-\frac{R}{\lambda}}]$$

If this is divided by GM_S and the following definitions are made,

$$\begin{aligned} \mu &\equiv \frac{M_E}{M_S} \\ A &\equiv [1+\alpha(1+\frac{r}{\lambda})e^{-\frac{r}{\lambda}}] \end{aligned}$$

then the equation becomes

$$A = \frac{r^3}{(r+R)^3}[1+\alpha(1+\frac{r+R}{\lambda})e^{-\frac{r+R}{\lambda}}] + \frac{\mu r^3}{R^2(r+R)}[1+\alpha(1+\frac{R}{\lambda})e^{-\frac{R}{\lambda}}]$$

The goal now is to group this equation by powers of R. Multiplication by $R^2(r+R)^3$ and some algebraic manipulation will yield the equation

$$\begin{aligned} R^5 \quad & +(3r)R^4 + (-\frac{\alpha r^3}{\lambda A}e^{-\frac{r+R}{\lambda}} - \frac{\mu\alpha r^3}{\lambda A}e^{-\frac{R}{\lambda}} + 3r^2)R^3 + (-\frac{r^3}{A} - \frac{\alpha r^3}{A}e^{-\frac{r+R}{\lambda}} \\ - \quad & \frac{\alpha r^4}{\lambda A}e^{-\frac{r+R}{\lambda}} - \frac{\mu r^3}{A} - \frac{\mu\alpha r^3}{A}e^{-\frac{R}{\lambda}} - \frac{2\mu\alpha r^4}{\lambda A}e^{-\frac{R}{\lambda}} + r^3)R^2 \\ + \quad & (-\frac{2\mu r^4}{A} - \frac{2\mu\alpha r^4}{A}e^{-\frac{R}{\lambda}} - \frac{\mu\alpha r^5}{\lambda A}e^{-\frac{R}{\lambda}})R + (-\frac{\mu r^5}{A} - \frac{\mu\alpha r^5}{A}e^{-\frac{R}{\lambda}}) = 0 \end{aligned}$$

This may then be simplified into its final form

$$R^5 \quad +(3r)R^4 + \{ -\frac{\alpha r^3}{\lambda A}[e^{-\frac{r+R}{\lambda}} + \alpha e^{-\frac{R}{\lambda}}] + 3r^2\}R^3 + \{ -\frac{r^3}{A}[1 + \alpha(1 + \frac{r}{\lambda})e^{-\frac{r+R}{\lambda}}$$
$$+ \quad \mu(1 + \alpha(1 + \frac{2r}{\lambda})e^{-\frac{R}{\lambda}})] + r^3\}R^2 + \{ -\frac{\mu r^4}{A}[2 + \alpha(2 + \frac{r}{\lambda})e^{-\frac{R}{\lambda}}]\}R$$
$$-\frac{\mu r^5}{A}(1 + \alpha e^{-\frac{R}{\lambda}}) = 0 \tag{2.4}$$

We now define the *shift* in the Lagrange point distance ΔR as

$$\Delta R = |R - R_o|$$

where R is the perturbed distance given by (2.4) and R_o is the unperturbed distance given in (2.1). Note that, in the limits of zero potential strength or infinite distance scale, equation (2.4) becomes the unperturbed equation for the L2 position, (2.1), and therefore $\Delta R = 0$. Obviously, when the scalar potential is zero, the results of Newtonian gravity are unchanged. But the shift in the distance goes to zero as λ goes to infinity as well because the perturbed potential becomes

$$V(r) = -\frac{G(1+\alpha)M_1M_2}{r}e^{-\frac{r}{\lambda}}$$

and the scalar potential essentially amounts to a change in the gravitational constant; this effect is cancelled out in the calculation.

2.3 Analysis and Results

In order to find the perturbed L2 point, it is necessary to find the zeroes of equation (2.4). Since it cannot be solved analytically, we wrote a computer program which finds the L2 point (see Appendix A) and obtained a few sample data points, shown in the table below.

As can be seen in figure 2.1, an expected linear relationship exists between the potential strength and the L2 shift produced for a fixed distance scale. Unfortunately, it is clear from the results that the presence of even a strong fifth force has little effect.

Distance Scale (km)	Potential Strength	Distance Shift (km)
1×10^5	1×10^{-6}	$0(< 4.7 \times 10^{-5})$
1×10^7	1×10^{-6}	$4.968 \times 10^{-}1$
1×10^5	1×10^{-5}	$0(< 4.7 \times 10^{-5})$
1×10^6	1×10^{-5}	2.799
1×10^7	1×10^{-5}	4.97
1×10^5	1×10^{-4}	2.47×10^{-4}
5×10^5	1×10^{-4}	9.98
1×10^6	1×10^{-4}	2.798×10^1
1×10^7	1×10^{-4}	4.968×10^1

Table 2.1: L2 shifts at various scalar potential strengths and distance scales

Although WMAP orbits the L2 point, it would be nearly impossible to discern any effect that a scalar potential would have on the satellite. This is primarily because solar radiation pressure would have a much greater effect on any object placed near the L2 point. This effect, caused by the momentum of electromagnetic radiation emanating from the Sun, has a strength of

$$\frac{F_R}{F_G} = (5.78 \times 10^{-5})\frac{1}{\rho r}$$

where ρ is the matter density in kilograms per cubic meter and r is the radius of the affected object in meters[23]. Meanwhile, the scalar force ratio is given by

$$\frac{F_S}{F_G} = \alpha(1 + \frac{r}{\lambda})e^{-\frac{r}{\lambda}}$$

For distance scales between 100 thousand and 100 million kilometers, acceptable scalar strengths are *at most* between 10^-10 and 10^-8. So the radiation pressure will greatly overpower the scalar potential, and we must conclude that this method of constraining the scalar potential will not lead to better results than have already been seen.

The only way that these measurements could possibly of any value was if they were taken by a large, very high density object; this would minimize the effect of

the radiation. To illustrate this point, consider a distance scale on the order of the distance from the L2 point to the Earth. Then we may make the approximation

$$\frac{F_S}{F_G} \approx \frac{2\alpha}{e} \approx \alpha$$

If we want to significantly improve upon the current bounds, we would need to consider potential strengths around 10^{-10}. Because the effect of the scalar field will likely be very minute at this strength (around 5 centimeters), we will likely need to ensure that the radiation pressure produces a much smaller effect than the proposed potential. If we sent a spherical iron satellite with a mass density of $2500\frac{kg}{m^3}$ to the L2 point, it would need to have a radius of about 2300 meters to keep the force due to the radiation pressure one order of magnitude lower than the scalar effect. Since it does not seem feasable to send an iron satellite with a volume of 51 cubic kilometers and a mass of 55 billion kilograms containing sensors able to detect five centimeter shifts in the central point of its orbit around L2, we must conclude that this is not a very good way to constrain fifth-force potentials.

Chapter 3

Calculation of $< \dot{\omega} >$ of B1913+16 Due to a Scalar Potential

3.1 Important Concepts from Orbital Mechanics

In the previous section, we considered the nearly-circular orbit of the Earth around the Sun. This section deals with the elliptical orbits of a binary star system, which is a little bit more complicated. A few preliminary remarks on orbital mechanics should therefore be made.

In general, if a body is in a bound orbit around a central body due to a Newtonian gravitational potential, the equation which relates its radial distance from the center r to its angular position θ is [9]

$$r = \frac{a^2(1-e^2)}{(1+e\cos\theta)}$$

This is the equation of an ellipse where the central body is at one focus. The quantity a is called the *semimajor axis* and is the average distance of the orbiting body from the central mass. The *eccentricity* e of the orbit can be thought of as how elliptical the orbit is; when $e = 0$, the orbit is circular. We also see that $\theta = 0$ has been defined as the point in the orbit where the orbiting body is the closest to the central body. This point of closest approach is called the *periastron* of the orbit. At this point,

$$\theta = 0$$

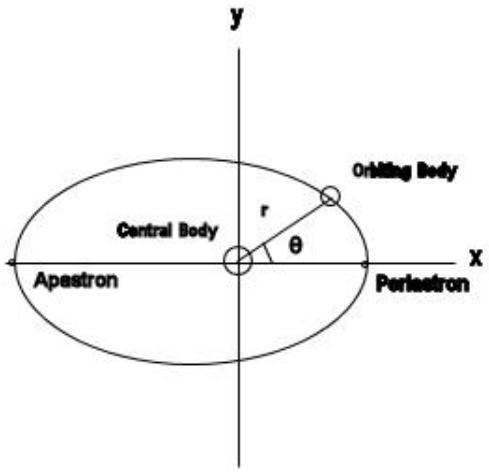

Figure 3.1: An elliptical orbit

$$r = a(1-e)$$

At the opposite end of the orbit is the point farthest from the central mass; this is called the *apastron* of the orbit. At the apastron,

$$\theta = \pi$$

$$r = a(1+e)$$

We will show that in the presence of a scalar potential, the orbit ellipse will rotate in the plane and the angle describing the periastron's location will change over time.

3.2 Introduction to Pulsars and Binary Pulsars

The objects that we will be studying are called *pulsars*. Pulsars are a type of neutron star that rotate extremely rapidly and emit a beam of radiation along their magnetic axis[15][23]. An observer on Earth with a radio telescope pointed at it will measure intermittent radio pulses between 0.002 and 4 seconds.

When a star between 1.4 - 3 solar masses can no longer sustain a fusion reaction because it is composed of virtually nothing but iron, there is no longer an outward pressure to prevent gravitational collapse, and it becomes a neutron star or a black hole. Angular momentum is conserved in this collapse, so

$$L = mvr \Longrightarrow v \propto \frac{1}{r}$$

This tells us that as the star's radius shrinks, its equatorial rotational velocity will increase. Because a star's radius will typically change from about 1 million kilometers to about ten kilometers, the increase in the rotation speed wil be enormous; some millisecond pulsars reach a rotation speed at their surface of about ten percent of the speed of light. These stars contain charged particles, and so their rotation creates a huge effective current. This current gives the pulsar an enormously powerful magnetosphere which directs charged particles (either pulled from the surface of the star by its huge electric field or captured from a nearby star) onto its magnetic dipole axis. These particles are unable to escape the magnetosphere except along this magnetic axis; this is what causes the radiation beam. Typically, the magnetic axis is inclined with respect to the rotational axis, so the beam will rotate around as the star itself rotates. If the beam is aligned with the Earth during part of its rotation, then an observer will detect very rapid, extremely regular pulses from that star's direction; this effect is often compared to a lighthouse. Figure 3.2 is a diagram of the structure of a pulsar; similar diagrams and further information may be found in the sources [15] [23].

An observer on Earth will be able to discern various properties of the pulsar by studying the properties, frequencies, and period of the detected pulses. But in the case of an orbiting pulsar, they are also very useful for obtaining orbital parameters.

A *binary pulsar* is a system of two stars orbiting one another in which one or

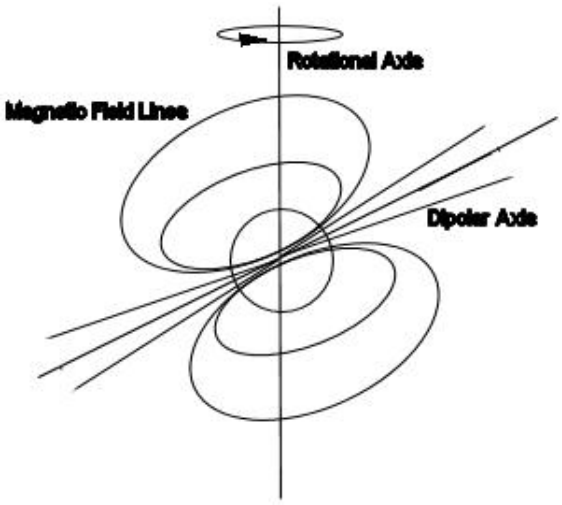

Figure 3.2: The structure of a pulsar

both of these stars are pulsars. The first binary pulsar was discovered by Hulse and Taylor in 1975 [21] and is named B1913+16. Only one of the stars in this system is a pulsar; the other is probably a white dwarf due to its smaller size. Using specialized equipment at Princeton University, Taylor *et. al.* have been recording the arriving pulses from the system over a very long period of time. The minute differences in these pulses over time have allowed them to discern the properties of the pulsar's orbit around its companion (see Appendix B). Because the two objects rotate around a fixed center of mass, the companion star's orbit is simply the same ellipse scaled according to the ratio of its mass to the pulsar mass.

The binary pulsar is particularly interesting because it serves as a test of General Relativity. Two relativistic effects that are important are the *precession of the periastron* and *gravitational radiation*[3]. General Relativity gives the following expression for the precession of an orbit's periastron $\Delta\phi$

$$\Delta\phi = \frac{6\pi G^2 M^2}{L^2}$$

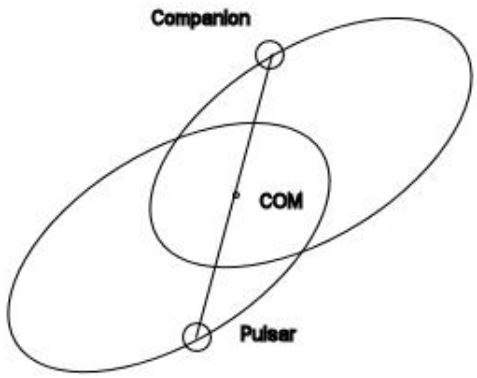

Figure 3.3: The binary pulsar system

This is derived for a body orbiting around a central mass, but we expect the periastron of the binary system to precess because the masses of the stars are huge compared to their angular momentum. Taylor *et. al.* have used thier observations to confirm this prediction of General Relativity.

Gravitational radiation is similar to electromagnetic radiation in many ways. Electromagnetic radiation is caused by electric charge being accelerated by electromagnetic forces. And when gravitational charge (mass) is accelerated by gravity, it emits gravitational radiation. The particularly large accelerations keeping the stars in orbit around each other makes the binary pulsar a particularly strong source of gravitational radiation. This radiation carries energy, and so the orbit loses this radiated energy over time. The result is that the two stars inspiral towards each other and the period of the orbit decreases. Eventually the two stars will collide at their center of mass. Taylor *et. al.* have observationally confirmed that the average rate of the period's decrease is correctly predicted by General Relativity.

A side effect of relativity is that the pulses arrive with a varying delay over the pulsar's orbit. This is an effect of the gravitational redshift of the pulses and of time dilation due to the speed of the stars. This effect and the two described above are all mass-dependent [22], and the intersection of the three curves shown in Figure 3.4 gives the observational value of the mass of the pulsar and its companion. This determination of the masses is what creates the constraint on the strength of a scalar potential, as we shall discover in the next section.

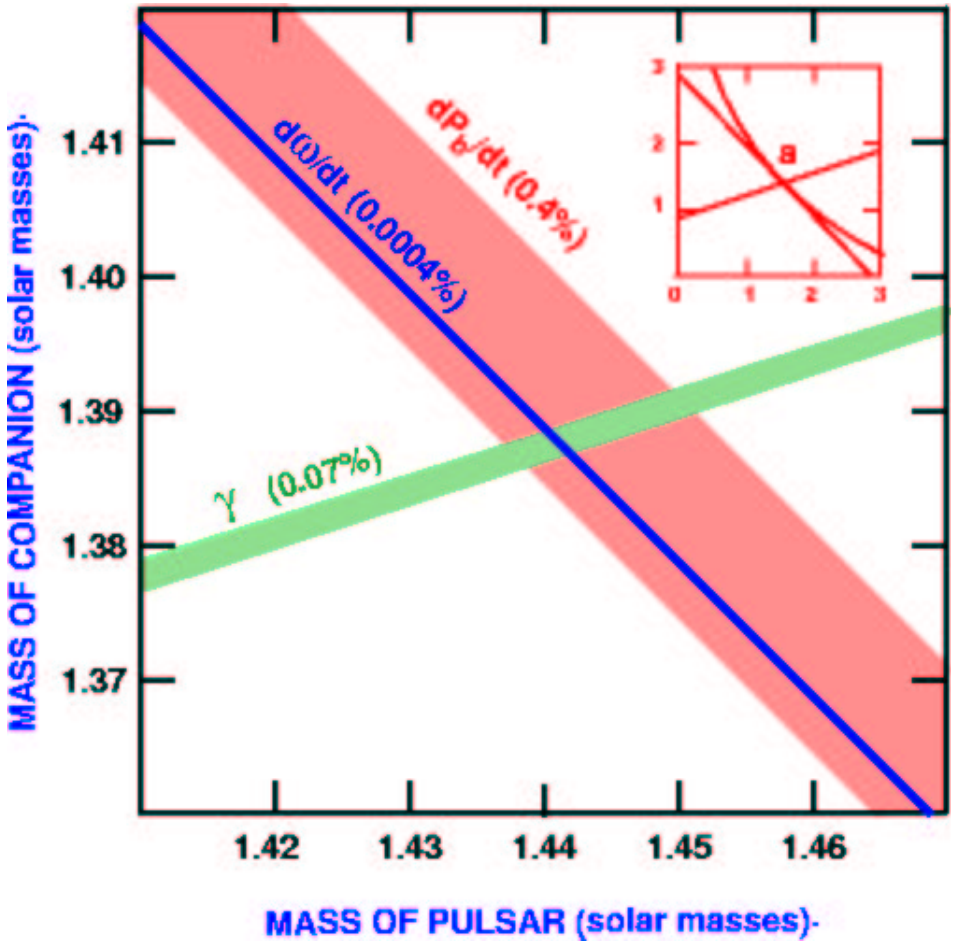

Figure 3.4: Determining the masses of the stars in B1913+16 [22]

3.3 Calculating the Periastron Shift

Our overall goal in this calculation is to obtain an expression for the change in the angular position of the rotating bodies with respect to a change in their distance coordinate. This expression may then be integrated over the orbit from the periastron to the apastron to obtain the total change in the angle over one orbit. For normal Newtonian gravity, the total angular change will be 2π — over one orbit, the orbiting bodies will make a complete revolution and return to the original periastron location. But if the potential energy of the system is perturbed slightly, we will find that the total angular change will be slightly different than 2π. This means that the mass indeed returns to the periastron location, but this position has been rotated slightly on the orbital plane. So this effect also causes the system's periastron to precess, but since both are perturbative effects, they are independent to first order. We therefore say that the total rate of change of the periastron angle is approximately the sum of the precession rate due to General Relativity and the precession rate due to the scalar potential. In other words, the presence of a scalar potential will shift the $\frac{d\omega}{dt}$ curve in figure 3.4. The constraint on the scalar potential is therefore that it cannot shift the curve for the periastron precession $\frac{d\omega}{dt}$ beyond the curve for the rate of period decrease $\frac{dP_b}{dt}$. If it did, there would be two separate intersection points for the three curves and the masses of the stars would be indeterminate. So in order to find this constraint, we need to calculate the scalar potential strength that will shift the $\frac{d\omega}{dt}$ curve to the very edge of the $\frac{dP_b}{dt}$ curve at each distance scale.

Because we are dealing with a two-body problem in which each body is of roughly equal mass, it is easiest to perform this calculation in the center of mass frame. Define a vector $\vec{r}$ as

$$\vec{r} = \vec{r_p} - \vec{r_c}$$

where $\vec{r_p}$ is the vector from the center of mass to the pulsar, and $\vec{r_c}$ is the vector from the center of mass to the companion star. If we define the *reduced mass* μ to be

$$\mu = \frac{m_p m_c}{m_p + m_c}$$

then the vector $\vec{r}$ will describe an orbit of the reduced mass around the center of mass that is a scaled version of the two separate orbits. This construction is simpler, and equivalent to, the more complex problem of two bodies orbiting each other.

We begin by considering the same type of scalar potential as before,

$$V_\alpha(r) = -\frac{\alpha G M m}{r} e^{-\frac{r}{\lambda}}$$

Adding this to the normal gravitational potential energy yields a total gravitational energy

$$V(r) = -\frac{G m_p m_c}{r}(1 + \alpha e^{-\frac{r}{\lambda}})$$

The force is therefore

$$\vec{F}(r) = -\vec{\nabla} V(r) = -\frac{d}{dr} V(r)\hat{r}$$

$$\vec{F}(r) = -\frac{G m_p m_c}{r^2}[1 + \alpha(1 + \frac{r}{\lambda})e^{-\frac{r}{\lambda}}]\hat{r}$$

Now the total energy of the orbit of the mass μ about the center of mass is given by

$$E = \frac{1}{2}\mu v^2 + V(r)$$

where v is the total velocity of μ. This velocity may be decomposed into a radial velocity and an angular velocity

$$E = \frac{1}{2}\mu[(\frac{dr}{dt})^2 + r^2(\frac{d\theta}{dt})^2] + V(r)$$

The angular momentum of the orbit is defined as

$$L = \mu r^2(\frac{d\theta}{dt})$$

Therefore, we may write the energy in terms of the angular momentum rather than the radial velocity

$$E = \frac{1}{2}\mu(\frac{dr}{dt})^2 + \frac{\mu r^2}{2}(\frac{d\theta}{dt})^2 + V(r)$$
$$E = \frac{1}{2}\mu(\frac{dr}{dt})^2 + \frac{L^2}{2\mu r^2} + V(r)$$

This can be solved for the time derivative of r, which gives us

$$(\frac{dr}{dt})^2 = \frac{2}{\mu}(E - V(r)) - \frac{L^2}{\mu^2 r^2}$$

Solving the angular momentum equation for the time derivative of θ yields

$$(\frac{d\theta}{dt})^2 = \frac{L^2}{\mu^2 r^4}$$

If we take these two expressions and divide the first by the second, we will obtain the derivative of r with respect to θ

$$(\frac{\frac{dr}{dt}}{\frac{d\theta}{dt}})^2 = (\frac{dr}{d\theta})^2 = (\frac{\mu^2 r^4}{L^2})[\frac{2}{\mu}(E - V(r)) - \frac{L^2}{\mu^2 r^2}]$$

When this is solved for $d\theta$, we get the equation we were looking for

$$d\theta = [\frac{2\mu r^4}{L^2}(E - V(r)) - r^2]^{-\frac{1}{2}} dr \tag{3.1}$$

The only problem now is that the energy and angular momentum of the orbit are unknowns; we need to find expressions for them.

We will first use some Lagrangian mechanics to find the angular momentum of the orbit. The Lagrangian $\mathcal{L}$ of the orbit is a quantity defined to be

$$\mathcal{L} = T - V = \frac{1}{2}\mu[(\frac{dr}{dt})^2 + r^2(\frac{d\theta}{dt})^2] - V(r)$$

where T is the kinetic energy of the orbit. The Euler-Lagrange equation for the minimum of the action gives us

$$\frac{d}{dt}(\frac{\partial \mathcal{L}}{\partial \dot{r}}) - \frac{\partial \mathcal{L}}{\partial r} = \mu\frac{d^2 r}{dt^2} - \mu(\frac{d\theta}{dt})^2 + \frac{dV(r)}{dr} = 0$$

By inserting L for $\frac{d\theta}{dt}$, we find

$$\mu(\frac{d^2r}{dt^2}) - \frac{L^2}{\mu r^3} = -\frac{\partial V(r)}{\partial r} = F(r)$$

Now, rearrangement of the equation for the angular momentum yields

$$\frac{d}{dt} = \frac{L}{\mu r^2}\frac{d}{d\theta}$$

and therefore

$$\frac{d^2}{dt^2} = \frac{L}{\mu r^2}\frac{d}{d\theta}(\frac{L}{\mu r^2}\frac{dr}{d\theta})$$

This is substituted into the expression above, and we subsequently define

$$u \equiv \frac{1}{r}$$

to obtain

$$-Lu^2\frac{d}{d\theta}(\frac{L}{\mu}\frac{du}{d\theta}) - (\frac{L^2}{\mu}u^3) = F(\frac{1}{u})$$

Putting the modified force into the equation and rearranging yields the following second-order differential equation —

$$(\frac{d^2u}{d\theta^2} + u) = \frac{\mu G m_p m_c}{L^2}[1 + \alpha(1 + \frac{1}{\lambda u})e^{-\frac{1}{\lambda u}}]$$

If we assume $\alpha << 1$ so that we may neglect the u-dependence on the right hand side of this equation, then the solution to this equation is

$$r = \frac{L^2}{\mu G m_p m_c[1 + \alpha(1 + \frac{r}{\lambda})e^{-\frac{r}{\lambda}}]}(\frac{1}{1 + e\cos(\theta + \theta')})$$

where we may choose $\theta' = 0$ by defining the line $\theta = 0$ to intersect the orbit at the periastron. This, of course, is the equation for the modified orbit. It is useful because by comparison to the standard Keplerian equation for the elliptical orbit[9]

$$r = \frac{a^2(1 - e^2)}{1 + e\cos\theta}$$

we see that

$$\frac{L^2}{\mu G m_p m_c[1+\alpha(1+\frac{r}{\lambda})e^{-\frac{r}{\lambda}}]} = a(1-e^2)$$

This leads immediately to an expression for the angular momentum in terms of known quantities

$$L^2 = \mu G m_p m_c a(1-e^2)[1+\alpha(1+\frac{r}{\lambda})e^{-\frac{r}{\lambda}}] \tag{3.2}$$

The next step is to find an expression for the energy. But instead of looking for an explicit expression, we will use the Virial Theorem, which states that for this bounded system in the unperturbed case

$$< T >= -\frac{< V >}{2}$$

where $< T >$ is the time-average of the system's total kinetic energy, and $< V >$ is the system's average kinetic energy. Energy conservation then implies

$$E =< T > + < V >= \frac{< V >}{2}$$

Because the perturbation is very small, we will simply add the average value of the perturbing term to the average gravitational potential in order to obtain the perturbed energy. Because the semimajor axis a is by definition the average value of r over the orbit, we find

$$E \approx \frac{< V(r) >}{2} \approx -\frac{G m_p m_c}{2a}(1+\alpha e^{-\frac{r}{\lambda}})$$

We have kept the r in the exponential for simplification; this will average to a later. So the quantity we need, $E - V(r)$, can be written

$$E - V(r) = G m_p m_c (1+\alpha e^{-\frac{r}{\lambda}})(\frac{1}{r} - \frac{1}{2a}) \tag{3.3}$$

We are now ready to calculate the shift in the periastron. When equation (3.3) is substituted into our expression for $d\theta$, equation (3.1) becomes

$$d\theta = [\frac{2\mu r^4}{L^2}(G m_p m_c(1+\alpha e^{-\frac{r}{\lambda}})(\frac{1}{r} - \frac{1}{2a})) - r^2]^{-\frac{1}{2}} dr$$

Now if we integrate dr from the periastron to the apastron twice, the equation above tells us that we will obtain the quantity $2\pi + \Delta\theta$ — the unperturbed (Newtonian) component of the integral will return 2π as expected, and the component proportional to the perturbation will generate the periastron precession $\Delta\theta$. This may be expressed as

$$2\pi + \Delta\theta = 2\int_{r_{pa}}^{r_{ap}} [\frac{2\mu r^4}{L^2}(Gm_p m_c(1+\alpha e^{-\frac{r}{\lambda}})(\frac{1}{r} - \frac{1}{2a})) - r^2]^{-\frac{1}{2}}\, dr$$

Simplification by inserting equation (3.2) and rearranging the result reduces this expression to its final form —

$$2\pi + \Delta\theta = 2a\sqrt{1-e^2}$$

$$\int_{r_{pa}}^{r_{ap}} \frac{1}{r}[\frac{1+\alpha(1+\frac{r}{\lambda})e^{-\frac{r}{\lambda}}}{(-r^2+2ar-a^2(1-e^2)) + \alpha e^{-\frac{r}{\lambda}}[r(2a-r) - a^2(1-e^2)(1+\frac{r}{\lambda})]}]^{\frac{1}{2}}\, dr \quad (3.4)$$

One more calculation needs to be performed — the periastron and apastron distances do not remain fixed in the presence of the perturbing potential. Hence the limits of integration in (3.4) are functions of α and λ. To see this, we first reduce the integral to its unperturbed form by setting $\alpha = 0$. Then $\Delta\theta = 0$ and we have

$$2\pi = 2a\sqrt{1-e^2}\int_{a(1-e)}^{a(1+e)} \frac{1}{r}\frac{1}{\sqrt{-r^2+2ar-a^2(1-e^2)}}\, dr$$

When the denominator is simplified, the integral becomes

$$2\pi = 2a\sqrt{1-e^2}\int_{a(1-e)}^{a(1+e)} \frac{1}{r}\frac{1}{\sqrt{(r-a(1-e))(a(1+e)-r)}}\, dr$$

The solution to an integral of this form is

$$\int_{r1}^{r2} \frac{1}{r}\frac{1}{\sqrt{(r-r1)(r2-r)}}\, dr. = \frac{\pi}{\sqrt{r1r2}}$$

so that the unperturbed integral gives

$$2a\sqrt{1-e^2}\int_{a(1-e)}^{a(1+e)} \frac{1}{r}\frac{1}{\sqrt{(r-a(1-e))(a(1+e)-r)}}\, dr = 2a\sqrt{1-e^2}(\frac{\pi}{\sqrt{a^2(1-e^2)}}) = 2\pi$$

and we see that the Keplerian orbit returns to its initial periastron position as expected. Notice that the endpoints of the integral were the roots of the quadratic in the denominator, or equivalently, points where $dr = 0$. We expect this because the periastron and apastron are the turning points of the orbit. The same will be true of the perturbed periastron and apastron, but they will be the roots of the quadratic expression in the perturbed integral (3.4).

We will approximate these perturbed endpoints by performing one iteration of Newton's method on the argument of the square root in (3.4). Defining this argument as $f(r)$, our approximation for the orbit endpoints x_1 will be

$$x_1 = x_0 + \frac{f(x_0)}{\frac{df(r)}{dr}\Big|_{r=x_0}}$$

where x_0 is the unperturbed orbit endpoint. Our function and its derivative are

$$\begin{aligned} f(r) &= (-r^2 + 2ar - a^2(1-e^2)) + \alpha e^{-\frac{r}{\lambda}}[r(2a-r) - a^2(1-e^2)(1+\frac{r}{\lambda})] \\ \frac{df(r)}{dr} &= 2(a-r) + \alpha[2ae^{-\frac{r}{\lambda}(1-\frac{r}{\lambda})} + re^{-\frac{r}{\lambda}}(\frac{r}{\lambda} - 2) + \frac{a^2r(1-e^2)e^{-\frac{r}{\lambda}}}{\lambda^2}] \end{aligned}$$

Dividing these two gives us a modification to x_0 which contains a term proportional to alpha in its denominator. We factor this out and then expand in α to obtain

$$\frac{f(r)}{\frac{df(r)}{dr}} = \frac{(-r^2 + 2ar - a^2(1-e^2)) + \alpha e^{-\frac{r}{\lambda}}[r(2a-r) - a^2(1-e^2)(1+\frac{r}{\lambda})]}{2(a-r)} \times$$

$$\{1 - \frac{\alpha[2ae^{-\frac{r}{\lambda}}(1-\frac{r}{\lambda}) + re^{-\frac{r}{\lambda}}(\frac{r}{\lambda} - 2) + \frac{a^2r(1-e^2)e^{-\frac{r}{\lambda}}}{\lambda^2}]}{2(a-r)}\}$$

However, because the unmodified periastron and apastron are the roots of the initial quadratic,

$$\Big(-r^2 + 2ar - a^2(1-e^2)\Big)\Big|_{r=\{a(1-e),a(1+e)\}} = 0,$$

there is only one term which is not of second-order and survives when we evaluate the expression at x_0. This term gives us

$$\frac{f(r)}{\frac{df(r)}{dr}} = \frac{\alpha e^{-\frac{r}{\lambda}}[r(2a-r) - a^2(1-e^2)(1+\frac{r}{\lambda})}{2(a-r)}$$

Plugging the orbit endpoints into our expression for x_1 produces our approximations for the perturbed periastron and apastron —

$$r_{pa} = a(1-e) + \alpha(\frac{a^2(1-e)(1-e^2)}{2\lambda e})e^{-\frac{a(1-e)}{\lambda}} \quad (3.5)$$

$$r_{ap} = a(1+e) - \alpha(\frac{a^2(1+e)(1-e^2)}{2\lambda e})e^{-\frac{a(1+e)}{\lambda}} \quad (3.6)$$

Our model for the periastron precession, expressed in equations (3.4), (3.5), and (3.6), has two compelling features. It correctly reduces to the unperturbed case in the limit $\alpha \to 0$, but the precession also vanishes when $\lambda \to 0$, as we can see from taking the limits

$$\lim_{\lambda\to\infty} r_{pa} = a(1-e)$$

$$\lim_{\lambda\to\infty} r_{ap} = a(1+e)$$

$$\lim_{\lambda\to\infty} 2\pi + \Delta\theta = 2\pi$$

This is entirely expected; as we noted in section 2.2, adding a scalar potential whose distance scale is infinite amounts to changing the gravitational constant to $(1+\alpha)G_o$ where G_o is the unperturbed constant. The total potential in this case remains inverse-square, and the result is the original Newtonian orbit. So we see that the derived model has the properties that we expect it to have. We must now evaluate the integral in (3.4) and compare the precession rate to the observational bounds in order to obtain the constraints on the scalar potential.

3.4 Numerical Analysis and Results

The integral in (3.4) cannot be evaluated analytically; we wrote a program in order to calculate it numerically (see Appendix A). This program exhibits all the correct properties; the distance scale going to infinity or the potential strength going to zero reduces to the unperturbed situation. The results of our calculations are in

table 3.1 and graphed in figure 3.5. Note that each value is based on a one million step approximation of the integral.

Potential Strength	Distance Scale (km)
2.2×10^{-3}	5×10^{4}
4.3×10^{-5}	7×10^{4}
1.3×10^{-5}	8×10^{4}
5.3×10^{-6}	9×10^{4}
2.5×10^{-6}	1×10^{5}
3.25×10^{-8}	5×10^{5}
3×10^{-8}	6×10^{5}
2.8×10^{-8}	7×10^{4}
2.8×10^{-8}	1×10^{6}
8.7×10^{-8}	1×10^{7}
7.3×10^{-7}	1×10^{8}
7.3×10^{-6}	1×10^{9}
7.3×10^{-5}	1×10^{10}
7.2×10^{-4}	1×10^{11}
3.6×10^{-3}	5×10^{11}

Table 3.1: Constraints on Scalar Potential Parameters

In figure 3.6, we compare the results obtained to the current constraints on a composition-independent Yukawa potential. Our results are not good enough to push the constraints significantly below the lunar precession or LAGEOS studies. Although the pulsar study does seem to outperform current planetary studies at very long distance scales, a determination of the precession rates of the outer planets would easily outperform the pulsar constraints. The main obstacle to achieving better bounds lies in the innacurate determination of the rate of period decrease (see Fig. 3.4). If this could be determined more accurately, the constraints would improve considerably. If the linewidth of the period measurement could be decreased to the same width as that of the periastron measurement, the constraints would probably improve by a couple orders of magnitude. This could make the binary pulsar system the best constraint

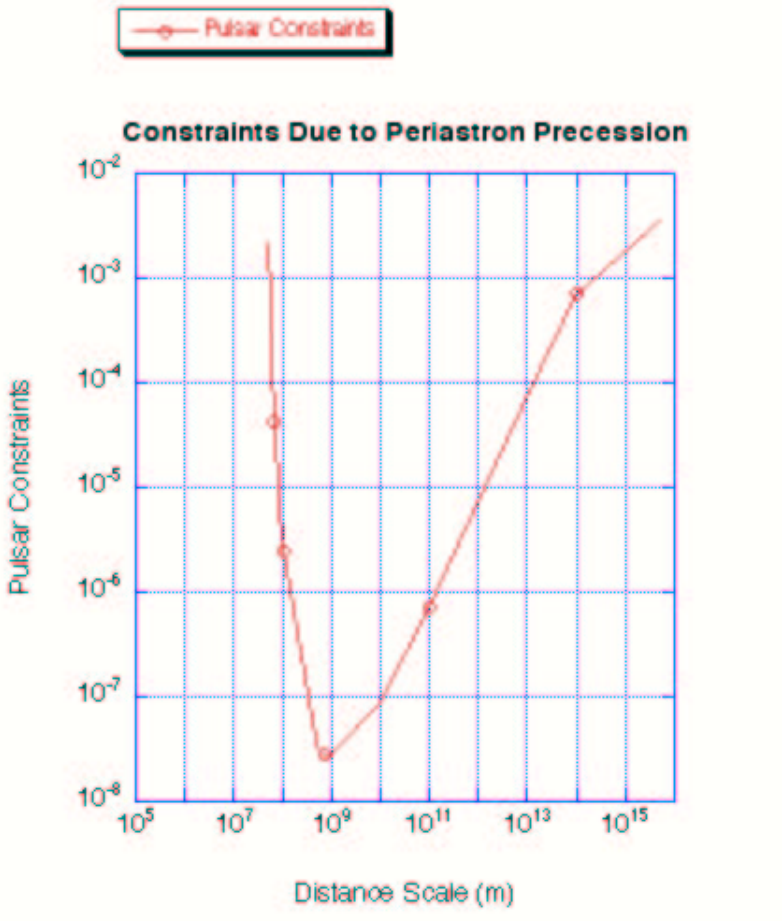

Figure 3.5: Constraint plot generated by periastron precession calculation

on a scalar potential for some distance scales in the near future.

3.5 Possibilities for Future Study

Things look very good for research into this area — many new binary pulsars are being discovered and the methods that are being used to investigate their properties are greatly improving [13]. Obviously, as the uncertainty in our observational data on these systems improves, so will the constraints on a perturbing potential. In addition, a binary pulsar system which is made up of *two* pulsars has been discovered

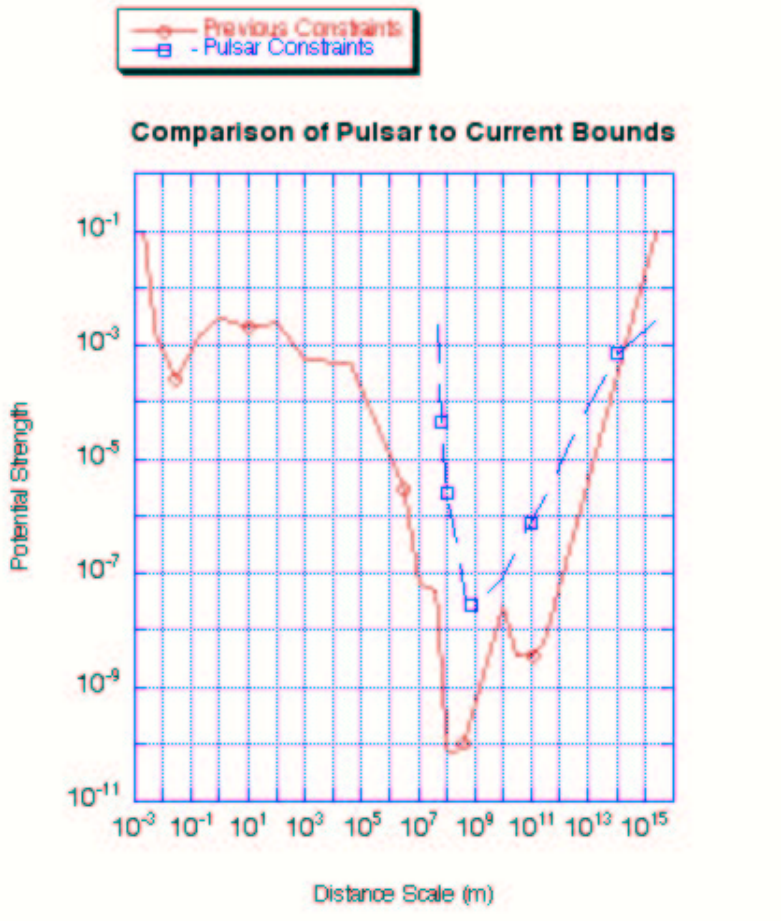

Figure 3.6: Comparison of pulsar constraint to current bounds

[14]. As the amount of incoming data from this system will be twice as great, we may obtain much better measurements of the orbital and post-Keplerian parameters than is possible with single-pulsar systems. Binary pulsars will be an important phenomena for future investigation in both fifth-force studies and learning about various other phenomena such as gravitational radiation.

Chapter 4

Analyis of a Composition-Dependent Force from an Galilean Free-Fall Experiment

4.1 Free-Fall Experiments

As we saw in the first chapter, getting limits on a fifth force at small distance scales generally involves performing a experiment here on Earth. In our study, we consider a free-fall experiment designed to test the Weak Equivalence Principle in laboratory distance scales. In the analysis of these experiments, the inertial and gravitational masses are taken to be distinct constants in the force equation,

$$m_i \frac{d^2y}{dt^2} = -\frac{Gm_g M_E}{y^2} = m_g g$$

where m_i is the inertial mass that governs the proportion between force applied and acceleration achieved and m_g is the gravitational mass, the constant that determines the force due to gravity on the mass. Equivalently, we may attribute this difference to the presence of a fifth force rather than to the inequality of gravitational and inertial mass:

$$m_i \frac{d^2r}{dt^2} = -\frac{Gm_g M_E}{r^2} = -\frac{Gm_i M_E}{r^2} - \frac{\alpha(1+\frac{r}{\lambda})Gm_i M_E}{r^2} e^{-\frac{r}{\lambda}}$$

Essentially, we are stating the gravitational mass in terms of the fifth force as

$$m_g = m_i(1 + \alpha(1 + \frac{r}{\lambda}))e^{-\frac{r}{\lambda}}$$

One may object that we are equating a constant to a function of the position. However, we may attribute this to a gravitational constant that is a function of the height of the object rather than to a changing mass.

Note that a force of this type is the result of the same potential as before;

$$V(r) = -\frac{G(1+\alpha)m_i M_E}{r}e^{-\frac{r}{\lambda}}$$

However, rather than simply consider a fifth force which couples to all matter identically, we are now examining a potential whose strength is composition-dependent. Our goal will be to take the experimental constraints placed on differential accelerations of test bodies and derive the limits on the strengths of these composition-dependent forces.

4.2 Description of Experiment and Results

The experiment we will use to derive limits was performed in 1992 by Carusotto *et. al.* [4]. To measure the difference in the accelerations of aluminum and copper in free-fall, they constructed a metal disk by combining two half-disks, one consisting of aluminum and the other of copper, and adding reflectors to the sides that were designed to reflect light along a path parallel to its fall. This disk was dropped (in a careful way) down an apparatus, at the base of which was a modified Michelson interferometer. Two laser beams were reflected up the apparatus to the falling disk then reflected back to photodiodes. The difference in the distance traveled by the two beams is related to the angular motion of the disk, and this allowed a measurement of the difference in the acceleration of the two sides.

In its analysis of the results, the study assumes a Yukawa potential that has different potential strengths for aluminum, α_{Al}, and copper, α_{Cu}. Based on their data, Carusotto *et. al.* conclude

$$|\lambda\Delta\alpha| \leq 0.50cm$$

where

$$\Delta\alpha \equiv \Delta\alpha_{Cu} - \Delta\alpha_{Al}$$

4.3 Limits Placed on a Force Coupling to Nucleons

Based on these findings, we wish to study a type of scalar potential which affects neutrons and protons differently. In general, the potential of this type on an atom due to the mass of the Earth is

$$V(r) = \frac{Gm_iM_E}{r} + \frac{\alpha_pGn_pm_pM_E}{r}e^{-\frac{r}{\lambda}} + \frac{\alpha_nGn_nm_nM_E}{r}e^{-\frac{r}{\lambda}}$$

where m_i is the inertial mass of the atom, n_n is the number of neutrons that the atom contains, n_p is the atomic number of the atom, m_n is the mass of a neutron, and m_p is the mass of a proton. Here α_p is the strength of the potential's coupling to protons and α_n is the strength of its coupling to neutrons. Because the experimental disk contains roughly the same masses of aluminum and copper and any difference in mass has been eliminated through the experimental method, we may simply study the limits on the differential accelerations of single atoms of copper and aluminum.

First, it is important to note that there are two principal naturally occuring isotopes of copper, CU-63 and CU-64. These isotopes are of equal abundance in nature, and we can only assume that they are of equal abundance in the experimental disk. Therefore, we will assign it an an atomic mass of 63.5 for statistical reasons. Now, in order to get Carusotto's results into a form useful for our purposes, we equate the

potential coupling to the individual elements with a potential coupling to protons and neutrons. For copper,

$$\frac{\alpha m_{Cu} M_E}{r} e^{-r\lambda} = \frac{\alpha_p n_{pCu} m_p M_E}{r} e^{-\frac{r}{\lambda}} + \frac{\alpha_n n_{nCu} m_n M_E}{r} e^{-\frac{r}{\lambda}}$$

which leads to

$$\alpha_{Cu} m_{Cu} = \alpha_p n_{pCu} m_p + \alpha_n n_{nCu} m_n$$

Copper's atomic number is 29 and its effective neutron number is therefore 34.5. Using these facts, we find that the expression for the coupling constant is

$$\alpha_C u = \frac{29\alpha_p m_p + 34.5\alpha_n m_n}{m_{Cu}}$$

A similar expression can be found for aluminum, with an atomic number of 13 and a neutron number of 14 —

$$\alpha_{Al} = \frac{13\alpha_p m_p + 14\alpha_n m_n}{m_{Al}}$$

These two equations are subtracted to find the expression for $\Delta\alpha$

$$\Delta\alpha = \frac{29\alpha_p m_p + 34.5\alpha_n m_n}{m_{Cu}} - \frac{13\alpha_p m_p + 14\alpha_n m_n}{m_{Al}}$$

$$\Delta\alpha = \frac{\alpha_p m_p (29 m_{Al} - 13 m_{Cu}) + \alpha_n m_n (34.5 m_{Al} - 14 m_{Cu})}{m_{Cu} m_{Al}}$$

Therefore the experimental constraint in terms of the neutron and proton coupling constants is

$$|\lambda\Delta\alpha| = |\lambda \frac{\alpha_p m_p (29 m_{Al} - 13 m_{Cu}) + \alpha_n m_n (34.5 m_{Al} - 14 m_{Cu})}{m_{Cu} m_{Al}}| \leq 5\times10^{-3} m \quad (4.1)$$

We now make use of the following readily-available facts

$$\begin{aligned} m_{Al} &= 4.516\times10^{-26} kg \\ m_{Cu} &= 1.062\times10^{-25} kg \\ m_p &= 1.6725\times10^{-27} kg \\ m_n &= 1.6748\times10^{-27} kg \end{aligned}$$

to simplify equation (4.1), which becomes

$$|\lambda(\alpha_n - 1.00138\alpha_p)| \leq 2.01706\times10^{-1}m$$

Because $\lambda > 0$ and the coefficient of α_p is just the ratio of the neutron mass to the proton mass, the final simplfied form of (4.1) is

$$|\alpha_n - \frac{m_n}{m_p}\alpha_p| \leq \frac{2.01706\times10^{-1}m}{\lambda} \tag{4.2}$$

This equation gives the maximum difference between the couplings to protons and neutrons at a given distance scale.

Two constraint equations are contained within (4.2), given by

$$\begin{aligned} \alpha_n &= \frac{m_n}{m_p}\alpha_p + \frac{2.01706\times10^{-1}m}{\lambda} \\ \alpha_n &= \frac{m_n}{m_p}\alpha_p - \frac{2.01706\times10^{-1}m}{\lambda} \end{aligned}$$

The coupling constants are constrained to fall within these lines. If we define the *characteristic separation* $\Delta\Psi$ to be the difference between the maximum and minimum allowed values of one parameter when the other is constant, it is easy to see that

$$\Delta\Psi = \frac{4.03412\times10^{-1}m}{\lambda} \tag{4.3}$$

This is a measurement of the allowed difference in the coupling constants. It is inversely proportional to λ, and so non-negligible differences in the coupling constants are only possible at very short distance scales.

A more formal analysis of this constraint requires that we change the parameters of the potential. We first define

$$\begin{aligned} \alpha_p &\equiv \alpha cos(\theta) \\ \alpha_n &\equiv \alpha sin(\theta) \end{aligned}$$

where α is the normal potential strength and θ is the *coupling angle*, which assigns the relative strength of the two coupling constants. Table 4.1 shows the relative strength of the two coupling constants and their relative difference at various coupling angles. The angle must be within $0 \leq \theta \leq \frac{\pi}{2}$ because the potential has to be attractive. The typical method is to express the constraints in terms of these parameters and the distance scale. Graphs of the constraints will assign constant values to either the distance scale or the mixing angle in order to show the constraints on the potential strength with respect to the other non-constant parameter. We will follow this convention in our analysis.

Rearrangement of the constraint equation (4.2) and use of the fact that the proton to neutron mass is approximately one yields

$$|sin(\theta) - cos(\theta)| \leq \frac{2.01706 \times 10^{-1} m}{\alpha\lambda}$$

and therefore

$$sin(\theta) - cos(\theta) \leq \frac{2.01706 \times 10^{-1} m}{\alpha\lambda} \text{ if } \theta > \frac{\pi}{4} \tag{4.4}$$

$$cos(\theta) - sin(\theta) \geq \frac{2.01706 \times 10^{-1} m}{\alpha\lambda} \text{ if } \theta < \frac{\pi}{4} \tag{4.5}$$

Notice that the constraint is discontinuous; no constraint exists for $\theta = \frac{\pi}{4}$ because the potential becomes composition-independent at that angle.

Figure 4.1 shows the constraints on the potential strength as a function of the angle for various distance scales. The strength must be below these curves; as we expect, this provides no constraint on a composition-independent potential. The strength scale is expressed in the usual way as a fraction of the Newtonian gravitational potential, so a strength of one means that at zero distance gravity is effectively doubled. We can see from this graph that any substantial composition-dependent effects are excluded beyond about 100m.

Figure 4.2 shows the potential strength constraint as a function of distance scale for various angles on a logarithmic plot. The strength must be above these curves. The following table illustrates the effect of the angle on the individual potential strengths α_p and α_n We see that as the angle moves away from $\frac{\pi}{4}$, the differentiation between

Angle (rad)	$\frac{\alpha_p}{\alpha}$	$\frac{\alpha_n}{\alpha}$	$\frac{\alpha_p}{\alpha} - \frac{\alpha_n}{\alpha}$
$\frac{7\pi}{32}$	0.773	0.634	0.139
$\frac{\pi}{5}$	0.809	0.587	0.222
$\frac{\pi}{6}$	0.866	0.5	0.366
$\frac{\pi}{8}$	0.924	0.382	0.542
$\frac{\pi}{10}$	0.951	0.309	0.642
$\frac{\pi}{16}$	0.981	0.195	0.786

Table 4.1:
Relative Coupling Strengths at Different Angles

the coupling constants increases. Turning to figure 4.2, we see that the effect of the angle moving away from $\frac{\pi}{4}$ is to increase the constraint on the potential strength at every distance scale. We conclude that the greater the difference in the interaction with protons and neutrons, the more constrained the potential strength.

4.4 Qualitative Study of Coupling to Quarks

In order to demonstrate that many different types of couplings may be studied simultaneously, we will carry the calculation in the previous section forward to qualitatively study couplings to quarks. We define α_u and α_d to be the couplings to the up quark and the down quark respectively. A proton is made of two up quarks and a down quark and a neutron is made of two down quarks and an up quark. Because the associated gluon fields will necessarily be included in any particle interactions with the quarks, we define each quark to be one-third of the mass of the associated nucleon.

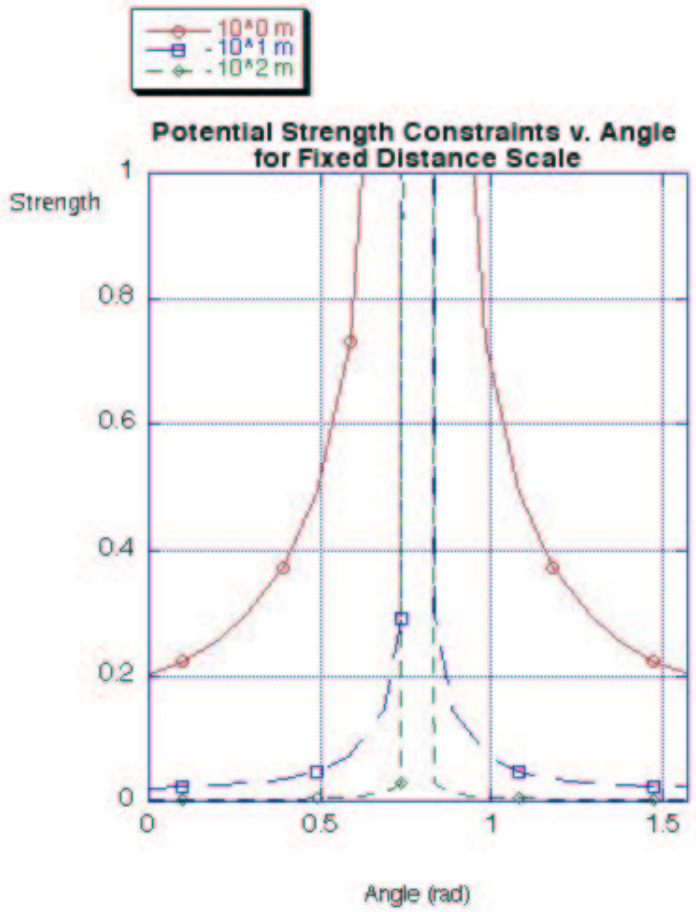

Figure 4.1: Constraints at fixed distance scales

We first define the new couplings in terms of the old, as before. The potentials in terms of the couplings to nucleons may be rewritten in terms of couplings to quarks:

$$\begin{aligned} \frac{\alpha_n G m_n M_E}{r} e^{-\frac{r}{\lambda}} &= \frac{G m_n M_E}{r} e^{-\frac{r}{\lambda}} \left(\frac{2\alpha_u}{3} + \frac{\alpha_d}{3}\right) \\ \frac{\alpha_p G m_p M_E}{r} e^{-\frac{r}{\lambda}} &= \frac{G m_p M_E}{r} e^{-\frac{r}{\lambda}} \left(\frac{2\alpha_d}{3} + \frac{\alpha_u}{3}\right) \end{aligned}$$

therefore,

$$\begin{aligned} \alpha_n &= \frac{2\alpha_u}{3} + \frac{\alpha_d}{3} \\ \alpha_p &= \frac{2\alpha_d}{3} + \frac{\alpha_u}{3} \end{aligned}$$

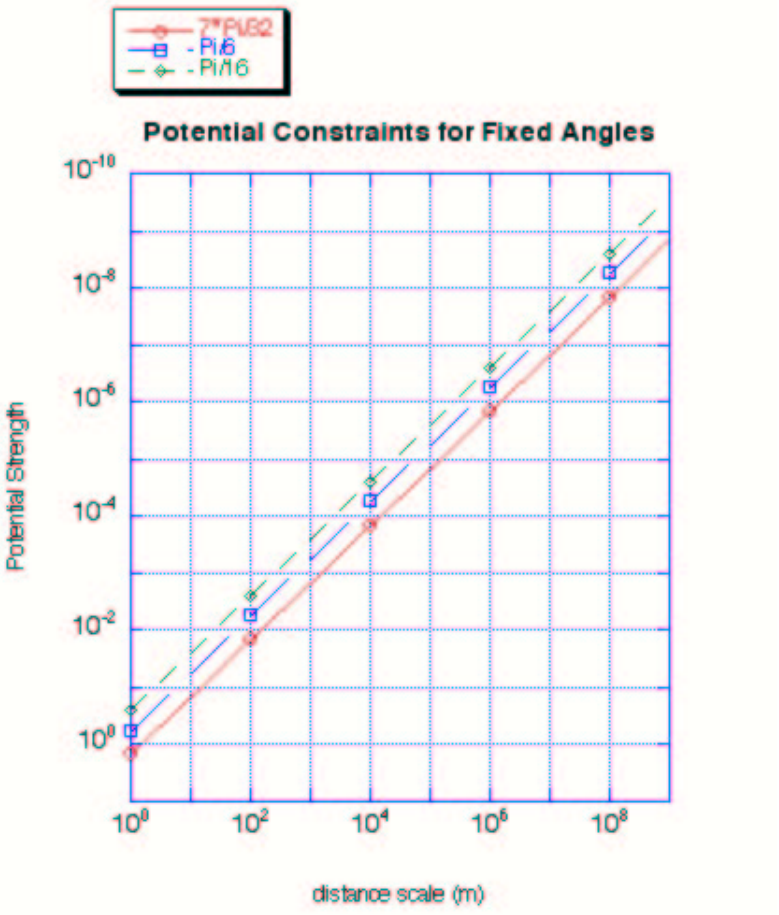

Figure 4.2: Constraints at fixed coupling angles

Substitution into (4.2) gives us

$$|\alpha_u - \alpha_d| \leq \frac{6.05118 \times 10^{-1} m}{\lambda} \tag{4.6}$$

By inspection of (4.6) we realize that the constraints on constituent particles scale as their individual mass. The quark constraints are three times weaker, giving us a characteristic separation of

$$\Delta\Psi = \frac{1.2102 \times 10^{0} m}{\lambda} \tag{4.7}$$

Equation (4.7) shows that as a result of the weaker constraints on the lighter particles, a significant difference in coupling constants is possible at greater distance scales. All

of the previous analyses of the nucleon coupling constraints will be identical for quarks except for the weakened constraint.

We have shown how it is possible to move from one set coupled objects to another to see how the constraints are different. A more sophisticated analysis would allow us to generate constraints which bound many different types of couplings with a relatively small amount of experimental data.

4.5 Possibilities for Future Study

Only one experiment involving two different types of substances was examined in this study. Further experiments involving many different types of substances would make our analyses much more statistically accurate. They would also give us systems with different properties like spin and nuclear composition to work with. If exotic matter were used in a differential acceleration experiment, even more interesting couplings could be studied. A few different pairings have already been studied [7], but more would be useful.

Appendix A

Computer Programs Used in Calculations

A.1 Program used in Calculation of L2 Shift

This program was used to find the zeroes of the quintic equation which describes the shifted position of the L2 Lagrange point. First, it asks for the value of the scalar potential and the distance scale, and then it takes a range of guesses for the shifted position and calculates the value of the equation for those guesses. After multiple tries, the guesses are made to converge around the zero of the equation corresponding to the shifted position. This procedure is then repeated for each combination of distance scale and potential strength.

```
//*****************************************************************************************
//  L2Table v1.0  by James Younkin
//  Date:  February 23, 2004
//  Purpose:  This program takes system parameters for the scalar potential and asks the user for
//            order to generate a table listing the values of the governing polynomial at each di
//  Input (from standard input):  The strength and distance scale of the scalar boson potential.
//                                limit, and number of entries to create the table
//  Output (to standard output):  The program will display a table listing the distance, shift fr
//                                and polynomial value for each table entry.
//*****************************************************************************************

#include <math.h>
#include <fstream.h>
#include <iostream.h>
```

```
#include <iomanip.h>

// Variable declarations
int i;                                                  // Counter used in program loops
char holder;                                            // Used for program pauses
double R_unpert;                                        // Unperturbed L2 distance in km
bool done_main;                                         // Governs main program loop
bool done_system;                                       // Governs system loop
int row_count;                                          // Used to display table in readable pi
int step_counter;                                       // Used to count to step_number
const double r = 149476000;                             // Sun-Earth distance in km
const double mu = 0.000002986;                          // mass ratio -- earth/sun
bool done_finish_choice;                                // Governs final choice menu
double distance_scale;                                  // Scalar potential distance scale
double strength;                                        // Strength of scalar potential
bool done_system_choice;                                // Governs system choice loop
bool done_calc;                                         // Governs calculation loop
double lower_bound;                                     // Smallest distance on table
double upper_bound;                                     // Largest distance on table
int step_number;                                        // number of steps to be performed
double step_size;                                       // Step size
double curr_distance;                                   // Current step distance
bool restart;                                           // Governs system restart loop
double fifth;                                           // R^5 piece of polynomial
double fourth;                                          // R^4 piece of polynomial
double third;                                           // R^3 piece of polynomial
double second;                                          // R^2 piece of polynomial
double first;                                           // R^1 piece of polynomial
double constant;                                        // constant piece of polynomial
double polynomial;                                      // polynomial value at curr_distance
double shift;                                           // shifted distance at curr_distance
double A;                                               // A function
char system_choice;                                     // Choice in system menu
char finish_choice;                                     // Choice in final menu

int main()
{
  // Initialize
  done_main = false;
  done_system = false;
  row_count = 0;


  // Clear screen / Introduction
  for(i=1;i<=50;i++)
    {
      cout <<  endl;
    } // for
  cout << "L2Table  by James Younkin" << endl;
  cout << "This program generates a table which allows the determination" << endl;
  cout << "of the distance shift in the L2 point in the presence of a" << endl;
```

```
cout << "scalar potential." << endl << endl;
cout << "Press any key followed by ENTER to continue";
cin >> holder;
for(i=1;i<=50;i++)
  {
    cout << endl;
  } // for

// Store unperturbed distance
R_unpert = 1500000;

// Begin main program loop
while(done_main==false)
{
  // Get system variables
  done_finish_choice = false;
  cout << "Please enter the strength of the scalar potential: " << endl;
  cin >> strength;
  cout << "Please enter the distance scale of the potential in km: " << endl;
  cin >> distance_scale;
  A = 1 + (strength*exp(-(r/distance_scale))*(1+(r/distance_scale)));
  done_system = false;
  done_system_choice = false;

  // Begin system loop
  while(done_system == false)
  {
    // Initialize
    step_counter = 0;
    row_count = 0;
    done_calc = false;
    done_system_choice = false;

    // Get table properties
     cout << "Please enter the lowest distance for the table in km: " << endl;
    cin >> lower_bound;
    cout << "Please enter the highest distance for the table in km: " << endl;
    cin >> upper_bound;
    cout << "Please enter the number of table entries you wish to produce: " << endl;
    cin >> step_number;
    step_number++;
    // Generate and display table
    step_size = (upper_bound - lower_bound)/(step_number - 1);
    curr_distance = lower_bound;

    while(done_calc==false)
      {
        for(i=1;i<=50;i++)
          {
            cout << endl;
          } // for
```

```
          row_count = 0;
          restart = false;
          cout << "*********************************************************************" << endl;
          cout << "*  Current Distance  *   Distance Shift   *      Polynomial    *" << endl;
          cout << "*********************************************************************" << endl;

          while(restart == false)
            {
              fifth = pow(curr_distance, 5);
              fourth = 3.0*r*pow(curr_distance, 4);
              third = ((-strength*pow(r, 3)*exp(-(r+curr_distance)/(distance_scale)))/(distance_
              second = (-(((pow(r, 3))/(A))*(1+(strength*exp(-(r+curr_distance)/(distance_scale)
              first = (-((2*mu*pow(r, 4))/(A)) - ((2*mu*strength*pow(r, 4)*exp(-(curr_distance)/
              constant = -((mu*pow(r, 5))/(A))  - ((mu*strength*pow(r, 5)*exp(-(curr_distance)/(
              polynomial = fifth + fourth + third + second + first + constant;
              shift = curr_distance - R_unpert;
              cout << "*" << setw(20) << curr_distance << "*" << setw(20) << shift << "*" << setw
              row_count++;
              step_counter++;
              curr_distance = curr_distance + step_size;
              if(step_counter == step_number)
                {
                  done_calc = true;
                  restart = true;
                  cout << "*********************************************************************" << e
                  cout << "Calculation complete." << endl;
} // if
              else if(row_count == 20)
                {
  restart = true;
  cout << "*********************************************************************" << endl << endl;
  cout << "Press any key followed by ENTER to continue" << endl;
  cin >> holder;
                } // else if
              else
                {
                } // else

            } // while

       } // while

      // Ask if the user wants to generate another table for the same system

      while(done_system_choice == false)
        {
          cout << "Do you want to generate another table for this system? (y/n)" << endl;
          cin >> system_choice;
          switch(system_choice)
            {
            case 'y': case 'Y':
```

```
            {
              done_system_choice = true;
              break;
            } // case
          case 'n': case 'N':
            {
              done_system = true;
              done_system_choice = true;
              cout << endl;
              break;
            } // case
          default:
            {
              cout << "That is not a valid choice!!" << endl;
            } // default
          } // switch
       } // while
    } // while
    // Ask if the user wants to restart with a new system
    while(done_finish_choice = false)
      {
        cout << "Would you like to create another system?" << endl;
        cin >> finish_choice;
        switch(system_choice)
          {
          case 'y': case 'Y':
            {
              done_finish_choice = true;
              break;
            } // case
          case 'n': case 'N':
            {
              done_main = true;
              done_finish_choice = true;
              cout << endl;
              break;
            } // case
          default:
            {
              cout << "That is not a valid choice!!" << endl;
            } // default
          } // switch
      } // while
  } // while
  cout << endl << "Thank you for using L2Table!" << endl;
  return 0;
} // int main()
```

A.2 Program Used in Calculation of $< \dot{\omega} >$ of B1913+16

This is the program which I used to calculate the precession of the periastron of the binary pulsar B1913+16. After the user inputs the parameters of the scalar potential, it asks for the number of steps to use in calculating the integral and the size of the buffer to use around the endpoints. Then the program performs the corresponding integral for the angular change in position of the periastron over one orbit using Simpson's rule. It outputs a menu listing the number of steps, potential strength, distance scale, step size, modified periastron and apastron distance, the total value of the integral, the angular change in the periastron over one orbit, and the angular change of the periastron over one year. Using this program is just a matter of adjusting the potential strength for a given distance scale until the periastron shift per year matches the observational limits.

There was an unfortunate problem with the program — the total unperturbed integral is about 10 percent off. We compensated for this by rescaling the periastron shift by $\frac{2*\pi}{5.619}$. Overall, this won't make much difference as the order of the constraints is not affected, but the constraints should only be interpreted as correct within $\approx$15%.

```
//*************************************************************************************
//  Periadvint v4.1  by James Younkin
//  Date:  April 10, 2004
//  Purpose:  To evaluate the sum for the advance of the periastron of the binary pulsar B1913+1
//            scalar boson potential.  The integral is calculated by subtracting the alpha = 0 in
//            alpha integral.  The integrals are calculated numerically using Simpson's Rule.
//  Input (from standard input):  The strength and distance scale of the scalar boson potential.
//                                of steps to be summed over.
//  Output (to standard output):  The program will output a table of the summation of the periast
//                                calculation progresses, and will output a summary of the calcul
//                                complete; the summary will include the input parameters, the su
//                                advance over one orbit, and the advance over one year.
//*************************************************************************************
```

```
#include <math.h>
#include <fstream.h>
#include <iostream.h>
#include <iomanip.h>

// Variable Declaration

int i;                                          // Variable used in program loops; clearing
char holder;                                    // Takes the buffer when program prompts fo
double strength;                                // The strength of the scalar potential
double distance_scale;                          // The distance scale of the potential in A
double step_number;                             // Number of steps for the calculation to b
bool done_main;                                 // Boolean for main program loop
bool done_calc;                                 // Boolean for calculation loop
const double periastron = 0.7466;               // Periastron separation in millions of ki
const double apastron = 3.1536;                 // Apastron separation in millions of kilo
double curr_distance;                           // Current distance for summation
double step_size;                               // Step size determined by step_number
int curr_step;                                  // Current step number for sum
bool done_choice;                               // Boolean governing final choice loop
char choice;                                    // Final choice for new calculation
double sum;                                     // Total sum of the calculation, to step
double sum_term;                                // Final summation term at the current dist
bool curr_step_even;                            // Boolean governing the application of Sim
double integral_buffer;                         // The distance from the endpoints that the
const double semimajor_axis = 1.9501;           // The semimajor axis of the unperturbed or
const double eccentricity = 0.6171338;          // The eccentricity of the unperturbed orbi
double periastron_prime;                        // The periastron in AU, modified for the p
double apastron_prime;                          // The apastron in AU, modified for the per
double periastron_new;                          // The effective periastron for the integra
double apastron_new;                            // The effective apastron for the integral
double g;                                       // The value of the function g at curr_dist
double numerator;                               // The term in the numerator of the integra
double denominator;                             // The term in the denominator of the integ
const double Pi = 3.14159265358979323846;       // The value of Pi
double orbit_mod;                               // The value of the correction for the peri
double endpoint_mod;                            // The value of the correction for the endp
double dg_dr_apastron_prime;                    // The value of the partial derivative of g
double dg_dr_periastron_prime;                  // The value of the partial derivative of g
double sqrt_term;                               // Variable used to help in final sum calcu
double total_sum;                               // Final value for periastron advance per c
double total_sum_year;                          // Value of periastron advance over one yea
double sum_prime;                               // The total value of the integral multipli
double linear_constant_g;                       // The constant coefficient of the linear t
double expon_r_lambda;                          // Defined to be exp(-curr_distance/distanc

int main()
{
  done_main = false;
```

```
// Clear screen / Introduction
for(i=1;i<=50;i++)
{
  cout <<  endl;
} // for
cout << "Periadvint v4.1  by James Younkin" << endl;
cout << "This program calculates the periastron advance of the binary
star system" << endl;
cout << "B1913+16 in the presence of a Yukawa potential of specified"
<< endl;
cout << "strength and distance scale." << endl << endl;
cout << "Press any key followed by ENTER to continue";
cin >> holder;
for(i=1;i<=50;i++)
{
  cout << endl;
} // for

// Begin main calculation loop
while(done_main == false)
  {
    done_choice = false;
    done_calc = false;

    // Ask for parameters
    cout << "Please enter the scalar potential strength:" << endl;
    cin >> strength;
    cout << "Please enter the scalar distance scale, in kilometers:"  << endl;
    cin >> distance_scale;
    distance_scale = distance_scale/1000000;
    cout << "Please enter the number of steps for the sum to" << endl;
    cout << "be taken over: (Note that the number of steps" << endl;
    cout << "should be even)" << endl;
    cin >> step_number;

    for(i=1;i<=50;i++)
    {
      cout << endl;
    } // for

    // Calculate the modified periastron and apastron
    periastron_prime = (semimajor_axis*(1.0-eccentricity))+(strength*exp((-semimajor_axis*(1.0
    apastron_prime = (semimajor_axis*(1.0+eccentricity))-(strength*exp((-semimajor_axis*(1.0+e
    periastron_new = periastron_prime;
    apastron_new = apastron_prime;

    // Initialize calculation parameters
    curr_distance = periastron_new;
    step_size = ((apastron_new - periastron_new)/(step_number-1));
    sum = 0;
    curr_step = 1;
```

```
curr_step_even = true;

// Begin calculation loop
while(done_calc == false)
  {

    // Calculate sum term ( integral over g(r,lambda) )
    expon_r_lambda = exp(-curr_distance/distance_scale);
    numerator = 1.0+(strength*(1.0+(curr_distance/distance_scale))*exp(-curr_distance/dista
    denominator = ((-pow(curr_distance, 2)+(2.0*semimajor_axis*curr_distance)-(pow(semimaj
    g = numerator/denominator;
    sum_term = (1.0/curr_distance)*pow(g, (1/2))*2.0*semimajor_axis*pow((1-pow(eccentricity

    // Modify sum term according to Simpson's Rule
    if( curr_step == 1 )
    {
    } // if
    else if( (curr_step_even == true) && (curr_step != step_number) )
    {
      sum_term = sum_term * 2.0;
      curr_step_even = false;
    } // else if
    else if( curr_step_even == false )
    {
      sum_term = sum_term * 4.0;
      curr_step_even = true;
    } // else if
    else if( curr_step == step_number )
      {
      } // else if

    // Add sum term to total sum
    sum = sum + ( (1.0/3.0)*(step_size)*(sum_term) );

    // Check to see if calculation is finished; otherwise continue
    if(curr_step == step_number)
      {
        done_calc = true;
        cout << "Calculation complete." << endl << endl << endl;
      } // if
      else
      {
        curr_distance = curr_distance + step_size;
        curr_step++;
      } // else
  } // while

// Modify the completed sum by multiplying by coefficient, find
delta_theta, find angular change per year
sum_prime = sum;
total_sum = sum_prime - 5.61911153622421974;
```

```
      total_sum_year = total_sum * 1130.04;

      // Make final calculations
      endpoint_mod = endpoint_mod * 1000000;
      step_size = step_size * 1000000;
      apastron_prime = apastron_prime * 1000000;
      periastron_prime = periastron_prime * 1000000;
      distance_scale = distance_scale * 1000000;
      for(i=1;i<=50;i++)
        {
          cout <<  endl;
        } // for
// Display calculation summary
cout << "CALCULATION SUMMARY" << endl;
cout << "******************" << endl << endl;
cout << "Scalar Potential Strength:               " << strength << endl;
cout << "Scalar Distance Scale:                   " << distance_scale << " km" << endl;
cout << "Modified Periastron Location:            " << periastron_prime << " km" << endl;
cout << "Modified Apastron Location:              " << apastron_prime << " km" << endl;
cout << "Integral Buffer:                         " << endpoint_mod << " km" << endl;
cout << "Number of Steps:                         " << step_number << endl;
cout << "Step Size:                               " << step_size << " km" << endl;
cout << "Total Value of Integral:                 " << sum << endl;
cout << "Total Value of Normalized Integral:      " << sum_prime << endl;
cout << "Total Periastron Advance, One Orbit:     " << total_sum << endl;
cout << "Total Periastron Advance, One Year:      " << total_sum_year << endl << endl;
cout << "Press any key followed by ENTER to continue.";
cin >> holder;

// Ask for new calculation
while(done_choice == false)
        {
          cout << "Would you like to begin a new calculation? (y/n)" << endl;
          cin >> choice;
          switch(choice)
          {
            case 'y': case 'Y':
            {
              done_choice = true;
              for(i=1;i<=50;i++)
              {
                cout << endl;
              } // for
              break;
            } // case
            case 'n': case 'N':
            {
              done_choice = true;
              done_main = true;
              cout << endl << "Thank you for using Periadvint v4.1!" << endl << endl;
              break;
```

```
            } // case
            default:
            {
              cout << "That is not a valid choice!";
              break;
            } // default
          } // switch
        } // while
    } // while
    return 0;
} // int(main)
```

Appendix B

Properties of the Binary Pulsar B1913+16

The Keplerian (classical) parameters of B1913+16 that are of interest to us are [12]

$$\begin{aligned} \text{pular mass} &\approx 1.441 M_{Sun} \\ \text{companion mass} &\approx 1.387 M_{Sun} \\ \text{semimajor axis} &= 1,950,000 km \\ \text{periastron distance} &= 747,000 km \\ \text{apastron distance} &= 3,153,600 km \\ \text{eccentricity} &= 0.617131 \\ \text{orbital period} &= 7.75 hr \end{aligned}$$

The post-Keplerian parameters of B1913+16 are [21]

$$\begin{aligned} \text{average periastron precession rate (due to GR)} &= 4.22661 \frac{deg}{yr} \\ \text{time dilation amplitude} &= 0.0043 s \\ \text{rate of period decrease} &= -2.4211 \times 10^{-12} \frac{s}{s} \end{aligned}$$

Given these parameters, the two stars will inspiral and collide in about 300 million years.

Bibliography

[1] Baker, Robert M.L., Jr. Astrodynamics: Applications and Advanced Topics. London: Acadmeic Press Inc., 1967.

[2] Boynton *et. al.* Search for an Intermediate-Range Composition-Dependent Force. Phys. Rev. Lett. 59, 1385-1389 (1987).

[3] Carroll, Sean M. Spacetime and Geometry: An Introduction to General Relativity. San Francisco: Addison-Wesley, 2004.

[4] Carusotto *et. al.*, Phys. Rev. Lett. 69, 1722-1725 (1992).

[5] De Rujula, A. On Forces Weaker than Gravity. Phys. Lett. B. 180, 213-220 (1986).

[6] Dickey, J.O. *et. al.* Lunar Laser Ranging: A Continuing Legacy of the Apollo Program. Science 265, 482-490 (1994).

[7] Fischbach, E. Reanalysis of the Eötvös Experiment. Phys. Rev. Lett. 56, 3-6 (1986).

[8] Fischbach, Ephraim and Talmadge, Carrick L. The Search for Non-Newtonian Gravity. 1st ed. New York: Springer-Verlag, 1999.

[9] Geyling, Franz. Introduction to Orbital Mechanics. Massachusetts: Addison-Wesley Publishing Company, 1971.

[10] Hoskins, J.K. Experimental Tests of the Gravitational Inverse-Square Law for Mass Separations from 2 to 105 cm. Phys. Rev. D. 32, 3084-3095 (1985).

[11] Hubler, B. *et. al.* Determination of the Gravitational Constant with a Lake Experiment: New Constraints for Non-Newtonian Gravity. Phys. Rev. D. 51, 4005-4016 (1995).

[12] Johnston, Wm. Robert. Johnston's Archive. [Online] http://www.johnstonsarchive.net/relativity/binpulsar.html. Last updated 2 Nov. 2002.

[13] Lange, Ch. *et. al.* Precision Timing Measurements of PSR J1012+5307. Mon. Not. R. Astron. Soc. **000**, 1-9 (2001).

[14] Lyne, A.G. *et. al.* A Double-Pulsar System: A Rare Laboratory for Relativistic Gravity and Plasma Physics. Science, vol. 303, 1153. 20 February 2004.

[15] Lyne, Andrew G. and Graham-Smith, Francis. Pulsar Astronomy. 2nd ed. Campbridge: Cambridge University Press, 1998.

[16] The Wilkinson Microwave Anisotropy Probe Homepage (2004). [Online] Available: http://map.gsfc.nasa.gov/index.html.

[17] NASA Information Page on LAGEOS Satellites (2004). [Online] Available: http://msl.jpl.nasa.gov/QuickLooks/lageosQL.html.

[18] Romaides, Anestis J. Second Tower Experiment: Further Evidence for Newtonian Gravity. Phys. Rev. D. 50, 3608-3613 (1994).

[19] Smith, David E. *et. al.* A Global Geodetic Reference Frame from LAGEOS Ranging (SL5.1AP). J. Geophys. Res. 90, 9221-9223, (1985).

[20] Spero, R. *et. al.* Test of the Gravitational Inverse-Square Law at Laboratory Distances. Phys. Rev. Lett. 44, 1645-1648 (1980).

[21] Weisberg, Joel M. and Taylor, Joseph H. The Relativistic Binary Pulsar B1913+16. Radio Pulsars, Proceedings of August 2002 meeting in Chania, Crete. ASP Conference Series, Vol. to be determined, 2003. M. Bailes, D.J. Nice, & S.E. Thorsett, eds.

[22] Will, C.M. The Confrontation between General Relativity and Experiment. Living Rev. Relativity 4, (2001), 4. [Online Article]: cited on 20 Mar 2004. http://www.livingreviews.org/lrr-2001-4will/.

[23] Zeilik, Michael and Gregory, Stephen A. Introductory Astronomy and Astrophysics. 4th ed. Thomson Learning, Inc., 1998.

[24] Zee, A. Quantum Field Theory in a Nutshell. Princeton: Princeton University Press, 2003.

[25] Zumberge, Mark A. Submarine Measurement of the Newtonian Gravitational Constant. Phys. Rev. Lett. 67, 3051-3054 (1991).